ZIRAT17 ANNUAL REPORT

Annual Report

Authors

Peter Rudling
ANT International, Mölnlycke, Sweden

Charles Patterson
Clovis, CA, USA

Ron Adamson
Fremont, CA, USA

Friedrich Garzarolli
Fürth, Germany

A.N.T. INTERNATIONAL®

Advanced Nuclear Technology International
Analysvägen 5, SE-435 33 Mölnlycke
Sweden

info@antinternational.com
www.antinternational.com

Disclaimer

The information presented in this report has been compiled and analysed by Advanced Nuclear Technology International Europe AB (ANT International®) and its subcontractors. ANT International has exercised due diligence in this work, but does not warrant the accuracy or completeness of the information. ANT International does not assume any responsibility for any consequences as a result of the use of the information for any party, except a warranty for reasonable technical skill, which is limited to the amount paid for this assignment by each ZIRAT/IZNA programme member.

Contents

1 Introduction (Peter Rudling)

The objective of the Annual Review of ZIRconium Alloy Technology (ZIRAT) and Information on Zirconium Alloys (IZNA) is to review and evaluate the latest developments in ZIRAT as they apply to nuclear fuel design and performance.

The objective is met through a review and evaluation of the most recent data on zirconium alloys and to identify the most important new information and discuss its significance in relation to fuel performance now and in the future. Included in the review are topics on materials research and development, fabrication, component design, and in-reactor performance.

Within the ZIRAT17/IZNA12 Program, the following technical meetings were covered:

- Jahrestagung Kerntechnik, Annual Meeting on Nuclear Technology, 22-24 May 2012, Liederhalle Stuttgart, Germany
- Top Fuel Reactor Fuel Performance Meeting, Manchester, UK, 2-6 September, 2012
- International Conference on Characterization and QC of Nuclear Fuels (CQCNF 2012), Feb 27-29 India

The extensive, continuous flow of journal publications is being monitored by several literature searches of worldwide publications and the important papers are summarised and critically evaluated. This includes the following journals:

- Journal of Nuclear Materials
- Nuclear Engineering and Design
- Kerntechnik
- Metallurgical and Materials Transactions A
- Journal of Alloys and Compounds
- Canadian Metallurgical Quarterly
- Journal de Physique IV
- Journal of Nuclear Science and Technology
- Nuclear Science & Engineering
- Nuclear Technology

The primary issues addressed in the review and this report is zirconium alloy research and development, fabrication, component design, ex- and in-reactor performance including:

- Regulatory bodies and utility perspectives related to fuel performance issues, fuel vendor developments of new fuel design to meet the fuel performance issues.
- Fabrication and Quality Control (QC) of zirconium manufacturing, zirconium alloy systems.
- Mechanical properties and their test methods (that are not covered in any other section in the report).
- Dimensional stability (growth and creep).
- Primary coolant chemistry and its effect on zirconium alloy component performance.

- Corrosion and hydriding mechanisms and performance of commercial alloys.
- Cladding primary failures.
- Post-failure degradation of failed fuel.
- Cladding performance in postulated accidents (Loss of Coolant Accident (LOCA), Reactivity Initiated Accident (RIA)).
- Dry storage.
- Potential Burnup (BU) limitations.
- Current uncertainties and issues needing solution are identified throughout the report.

Background data from prior periods have been included wherever needed. The data published in this Report is only from non-proprietary sources; however, their compilation, evaluations, and conclusions in the report are proprietary to ANT International and ZIRAT/IZNA members as noted on the title page.

The authors of the report are Dr. Ron Adamson, Mr. Friedrich Garzarolli, Dr. Charles Patterson and, and, Mr. Peter Rudling, President of ANT International.

The work reported herein will be presented in two Seminars: in Clearwater Beach, FL., USA (February 6–8, 2012), in St Julien, Malta, Europe (March 7–9, 2012).

The Term of ZIRAT17/IZNA12 started on February 1, 2012 and ends on March 31, 2013.

2 BU achievements and key fuel performance issues (Peter Rudling and Alfred Strasser)

2.1 Introduction

The objective of this section is to summarize the key performance issues that could affect fuel design, fabrication or operation of the nuclear fuel in the near term or the longer term. The information sources reviewed, screened and evaluated include nearly all the related publications and technical meeting presentations of the past, approximately 18 months and focuses primarily on extended BU data but also other key results are provided. The section is intended to be a guide to significant, current issues and provide an alert to items that could affect fuel related operations. The extensive volume of information involved limits the presentations to the most significant features and conclusions, and the reader is urged to refer to the referenced publications.

2.2 Trends in fuel operating conditions

2.2.1 General trends

Improved fuel reliability and operating economics are the driving forces for the changes in operating conditions, while maintaining acceptable margins to operating and regulatory safety limits. These are incentives for significant advances in materials technology, software for modelling fuel performance, sophisticated instrumentation and methods for post-irradiation examinations. Some of these advances in technology have increased the demands on fuel performance levels and put pressure on the regulatory bodies to license operations to increased BU levels. The types of changes in Light Water Reactor (LWR) operating methods intended to achieve improved safety and economics have not changed in the past years and still include:

- Annual fuel cycles extended to 18 and 24 months,
- Increased discharge BUs to 58 GWD/MT batch average exposures by higher enrichments, increased number of burnable absorbers in the assemblies and in Pressurized Water Reactors (PWRs) higher Li and B levels in the coolant, or enriched B in the coolant,
- Plant power uprates that range from 2 to 20%,
- More aggressive fuel management methods with increased enrichment levels and peaking factors,
- Reduced activity transport by Zn injection into the coolant,
- Improved water chemistry controls and increased monitoring,
- Component life extension with Hydrogen Water Chemistry (HWC) and Noble Metal Chemistry (NMC)/On Line Noble Chemistry (OLNC) in Boiling Water Reactors (BWRs).

2.2.2 Fuel cycles

Cycle lengths

The trend for increased fuel cycle lengths has come to a near "equilibrium" **in the US** with PWRs operating at an average of 500 Effective Full Power Days (EFPD) per cycle and BWRs an average of 620 EFPD per cycle, up to a maximum of about 680 days for PWRs and 720 days for BWRs. Nearly all the US BWRs are trending toward 24 month cycles. The older, lower power density PWRs have implemented the 24 month cycles, but fuel management limitations, specifically the reload batch sizes required, have limited implementation of 24 month cycles in the high power density plants. The economics of 24 month cycles tend to become plant specific since they depend on the balance of a variety of plant specific parameters. The potential economic gains for cycle extension have decreased in the US as the downtimes for reloading and maintenance procedures were significantly reduced.

Other countries that historically have had only one peak power demand per year in the winter, compared to the two summer and winter power peaks in the US, are also trending toward longer cycles as a result of changes in economics, maintenance practices and licensing procedures. PWRs are trending toward 18 month cycles in France, Belgium and Germany.

2.2.3 BU extension

The major incentive for extended BUs is the potentially improved fuel cycle economy. The improved economics depend in part on the decreased amount of spent FAs to be purchased and handled. This is balanced by the increased amount of uranium and enrichment services required. The economics of decreased assemblies could also be impacted by the much longer cooling times required for High Burnup (HB) and Mixed Oxide (MOX) fuels in spent fuel pools prior to on-site dry storage or transport to a storage facility as noted later.

The average batch BUs in US PWRs are currently in the range of 42-54 GWD/MT and in US BWRs in the range of 45-52 GWD/MT.

Some European plants operated in the 50-60 GWD/MT batch BU range and have designed to go to 62 GWD/MT in their current cycles in both PWRs and BWRs. This is feasible, in part, due to their greater margin to their regulatory BU limits. The maximum BU Lead Test Assemblies (LTAs) are in the range of 67 – 79 GWD/MT for both reactor types. BU ranges by countries are compared to their regulatory limits in Table 2-1.

In addition to potential technical issues, the two major constraints to higher BU are the regulatory limits noted in Table 2-1 and the 5% enrichment limit.

Detailed reports of HB performance are given in Section 2.6.

Table 2-1: Maximum BUs achieved vs. regulatory limits, (excludes LTAs).

	BU (GWD/MT)				
Country	**Batch**	**Assembly**	**Rod**	**Pellet**	**Regulatory limit**
USA	54	58	62	73	62.5 peak rod
Belgium		50-55			55 UO_2 assy., 50 MOX assy.
Czech Republic	51	56	61		60 peak rod
Finland	45.6	46.5	53		45 assy
France	47	51 UO_2 42 MOX			52 assy
Germany	58	62	68		65 assy
Hungary		50	62		
Japan	50	55	62		55 UO_2 assy., 45 MOX assy.
Korean Republic	46				60 rod
Netherlands	51.5	58	64.5		60 rod
Russia	60	65			
Spain	50.4	57.4	61.7	69	
Sweden	47	57.2	63.6		60 assy., 64 rod
Switzerland	58	60	65	71	80 pellet
Taiwan					60 rod (P), 54 assy. (B)
UK	44.3	46.5	50		55 pellet
Ukraine		50			

ANT International, 2011

2.3 Fuel reliability

2.3.1 Guidelines

The Fuel Reliability Program (FRP) of the Electric Power Research Institute revised the Fuel Reliability Guidelines: "Fuel Surveillance and Inspection" [Daum et al, 2012]. The objective of the revision was to provide guidance to nuclear plant operators for developing proactive fuel assessment, inspection and surveillance programs to:

- Identify margins in key fuel performance areas;
- Assess margins following
  - changes in fuel design, manufacture and operation and,
  - anomalous operating events
- Provide guidance on failed fuel action planning.

[Daum et al, 2012] states that:

- The goal of a successful fuel inspection and surveillance program is to ensure good fuel performance to prevent poor fuel performance.
- The information collected during healthy fuel inspections should aid fuel failure root cause analyses and evaluation of other non-failure performance issues.

2.4 New fuel designs

2.4.1 Westinghouse

2.4.1.1 BWR

The latest BWR fuel design from Westinghouse is SVEA-96 Optima3 was described by [Bergmann et al, 2012], as follows.

Measurements of the control blade interference with SVEA-96 Optima2/Optima3 channels friction force were performed. The channels were pre-deformed with sinusoidal axial shape to simulate channel bow. The friction force was measured for a wide range of gaps between the channels. The calibration of the coefficient of friction is shown in Figure 2-1.

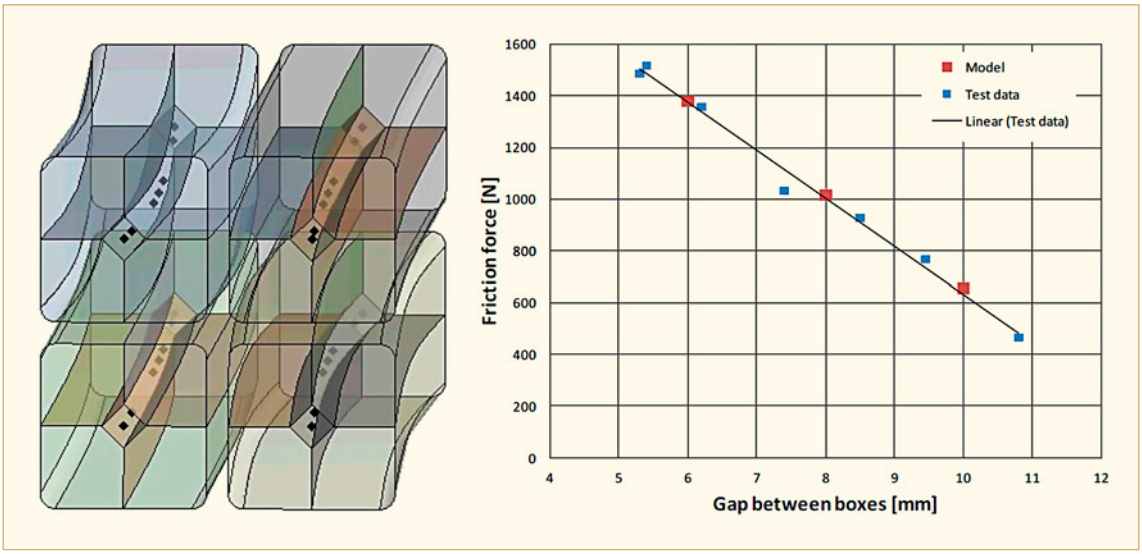

Figure 2-1: Left: ANSYS finite element model showing the bowing of 2x2 fuel channels in a control cell. Right: Comparison of the results for the ANSYS model with a friction coefficient μ=0.32 with experimental data from the Westinghouse BURE test loop [Bergmann et al, 2012].

It is easier to insert the CRs with bowed channels of the SVEA design than the GNF and AREVA fuel channel designs (Thick-thin designs), (Figure 2-2 and Figure 2-3). The CR/Channel friction force where channel distortion becomes an issue for the operation of the plant is somewhere in the range of 900 to 1800 N (200 to 400 lbs). The lower level is set by the gravitational force on the control rod acting during settle-time testing. The upper limit is the SCRAM limit that differs somewhat between plants. Based upon the calculations by [Bergmann et al, 2012], the authors conclude that the SVEA channel can bow at least 8 mm (assuming four channel sides interfering with the blade) without affecting plant operation. Recent channel bow measurements in Cofrentes NPP showed that a significant number of SVEA channels were bowing in the range from 8 to 11 mm towards the control rod without increasing the CR settle times, [Bergmann et al, 2012].

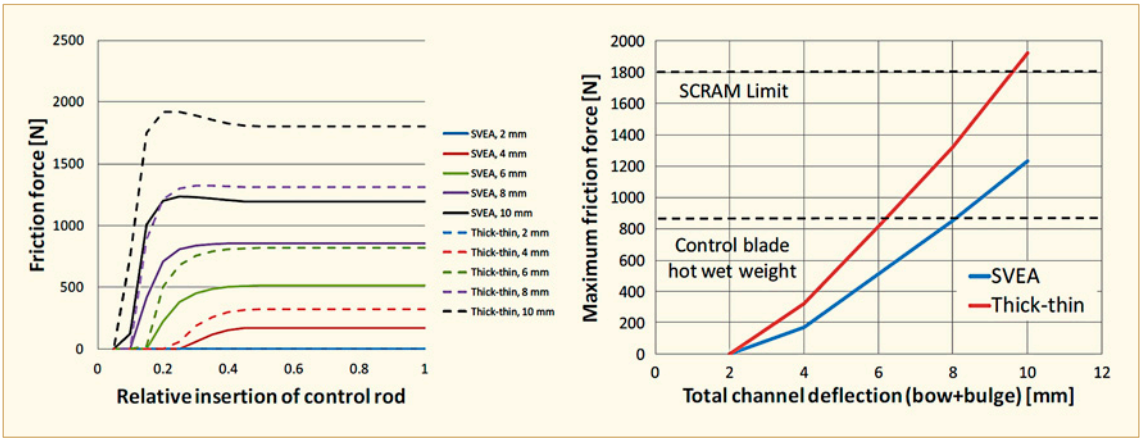

Figure 2-2: Left: Control rod friction force as function of CR insertion depth for different amounts of channel bow. Right: Maximum friction force (over CR insertion depth) as function of channel distortion (bow + bulge) [Bergmann et al, 2012].

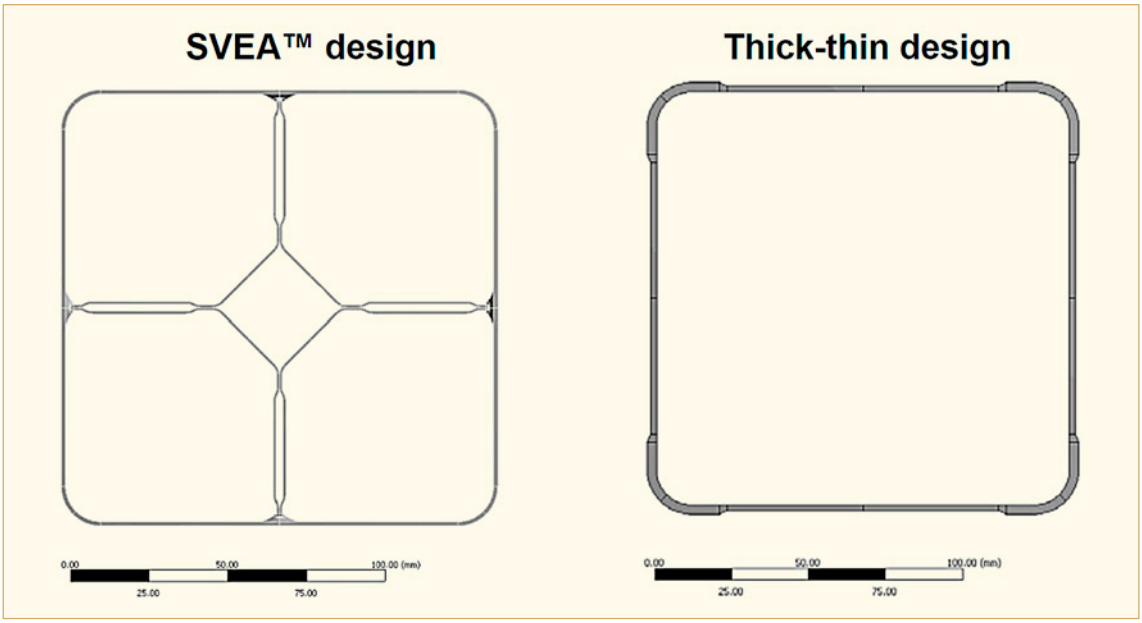

Figure 2-3: Fuel channel designs modelled with ANSYS code in 2x2 system with a control blade. Left: SVEA-96 Optima2 or Optima3. Right: Typical thick-thin design [Bergmann et al, 2012].

Other SVEA-96 Optima3 fuel design features according to [Bergmann et al, 2012] are:

- A new optimized spacer design (Figure 2-4) and the improved TripleWave+ debris filter (built from more sheets with thinner dimensions and an increased number of inlet "waves" than the previous TripleWave filter) to reduce debris fretting tendency. The objective of the designs was to ensure that any debris that is small or flexible enough to pass the debris filter will also pass the spacer.

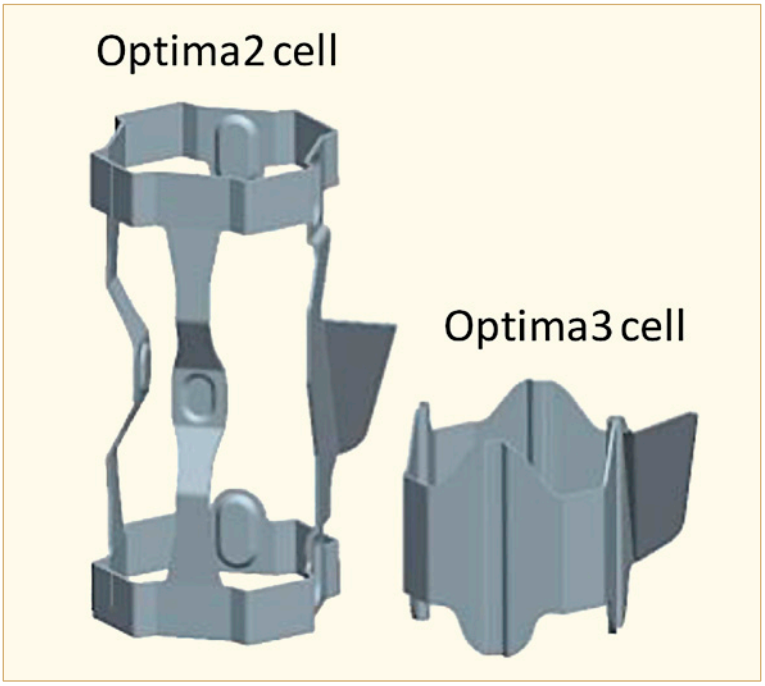

Figure 2-4: Spacer cells in SVEA-96 Optima and Optima [Bergmann et al, 2012].

- The Low-Tin ZIRLO channel show less susceptibility to fast neutron irradiation growth and shows lower levels of hydrogen pickup than standard Zry-2 and Zry-4 channel materials (Figure 2-5). *A lower irradiation growth vs. burnup slope reduces the amount of irradiation induced bow for a constant burnup/fluence gradient across the fuel channel.*

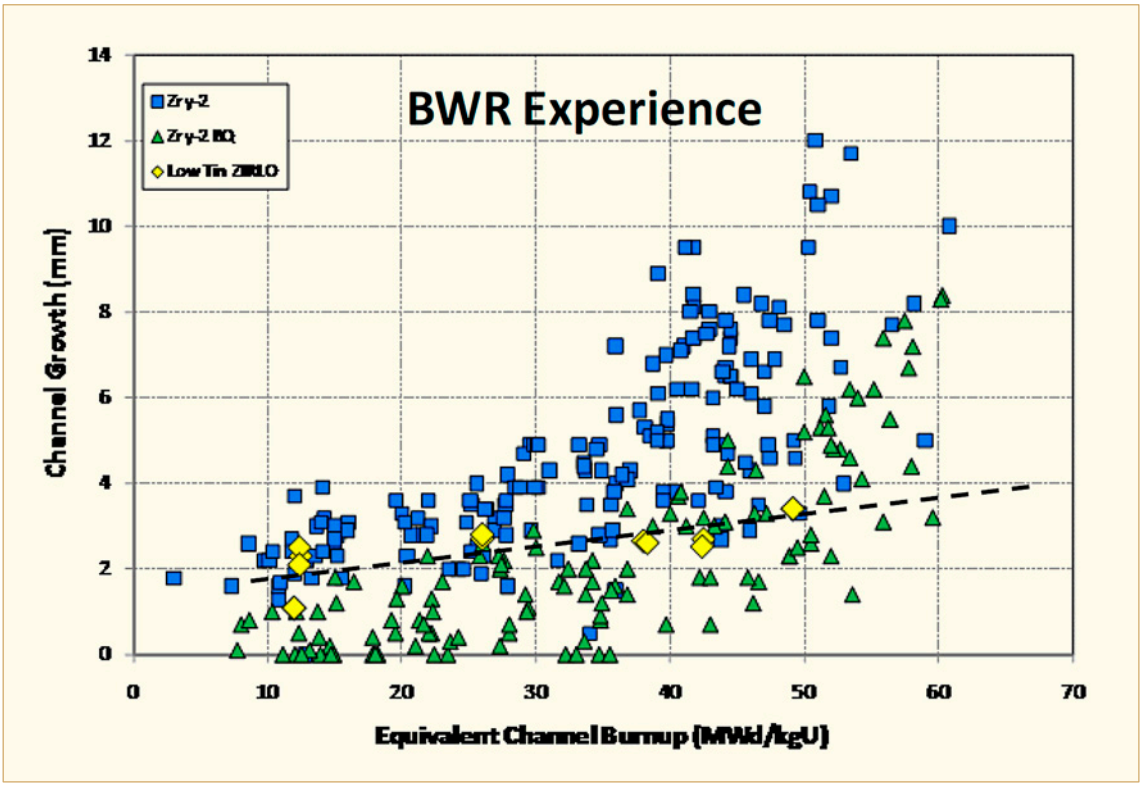

Figure 2-5: Westinghouse channel growth experience [Bergmann et al, 2012].

- Less parasitic neutron absorption than that of SVEA-96 Optima2, mainly due to its slim spacer design (Figure 2-4), but also due to the replacement of the helical plenum springs with spring clips.
- The slim spacer without protrusions also has significantly lower (two-phase) pressure drop. Combined with the TripleWave+ filter which increases (single-phase) pressure drop slightly at the assembly inlet, SVEA-96 Optima3 fuel provides better core stability.
- The overall assembly pressure drop is still significantly lower than in SVEA-96 Optima2.
- The critical power (where dryout occurs) is increased for the SVEA-96 Optima3 design.
- The heated rod length is increased with the introduction of freestanding rods (Figure 2-6), and slightly longer part-length rods. This provides lower average LHGR than in SVEA-96 Optima2. *The benefits of lower LHGR are several, e.g., reduction of FGR (i.e. increases the lift-off margin) and increased PCI margins.*
- The replacement of the top tie plate with a spacer allows for shorter end plugs. This in combination with the gain in space using the smaller spring clip yields 25% more plenum volume which reduces the end-of-life rod internal pressure by 10-15%, assuming the same fission gas release. *These feature increases the lift-off margins.*
- The high-density ADOPT pellet itself increases the uranium weight of the assembly by about 0.7%.

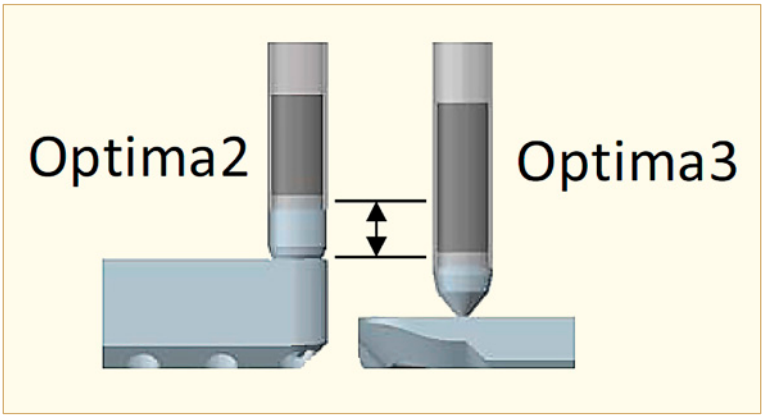

Figure 2-6: Thinner bottom tie plate with freestanding rods in SVEA-96 Optima [Bergmann et al, 2012].

2.4.1.2 PWR

A summary of various Westinghouse/ENUSA PWR designs is shown in Table 2-2.

Table 2-2: Summary of Westinghouse and ENUSA fuel design types, after [Bradfute et al, 2012].

Fuel type	W 17×17		W 15×15	W 14×14	CE 16×16	VVER
	RFA	OFA	Upgrade	422V+	NGF	
No. of plants	52	17	8	6	2	2
Fuel rod diameter (mm)	9.50	9.14	10.7	10.7	9.50	9.14
Mid-grid design	RFA-2	OFA	Upgrade	V+	NGF	VVER
IFMs	Optional	Yes	Yes	No	Yes	No
Top nozzle	Removable					
Cladding material	ZIRLO or optimized ZIRLO				Optimized ZIRLO	ZIRLO
Debris protection	DFBN, p-grid, oxide coating (US)			DFBN, oxide coating	Guardian	No
ANT International, 2010						

Most of the Westinghouse fuel designs have a multi-layer debris protection as illustrated in Figure 2-7. The Debris Filter Bottom Nozzle (DFBN) has small holes sizes to prevent debris from entering the assembly.

The Protective Grid (P-Grid) is located directly above the bottom nozzle and traps any debris that passes through the DFBN against the elongated solid-fuel-rod bottom end plug. In US fuel designs, a thin oxide coating is applied over the bottom six inches of each fuel rod to increase the cladding surface hardness.

The 17x17 and 15x15 designs operating in the US use all three levels of debris protection (Table 2-2). Fuel designs operating in Europe use the DFBN and P-grid.

The CE 16x16 NGF design uses the Guardian Grid to provide debris protection. This design, illustrated in Figure 2-8, uses a special grid at the bottom of the assembly along with a long end plug to trap debris and prevent it from entering the assembly.

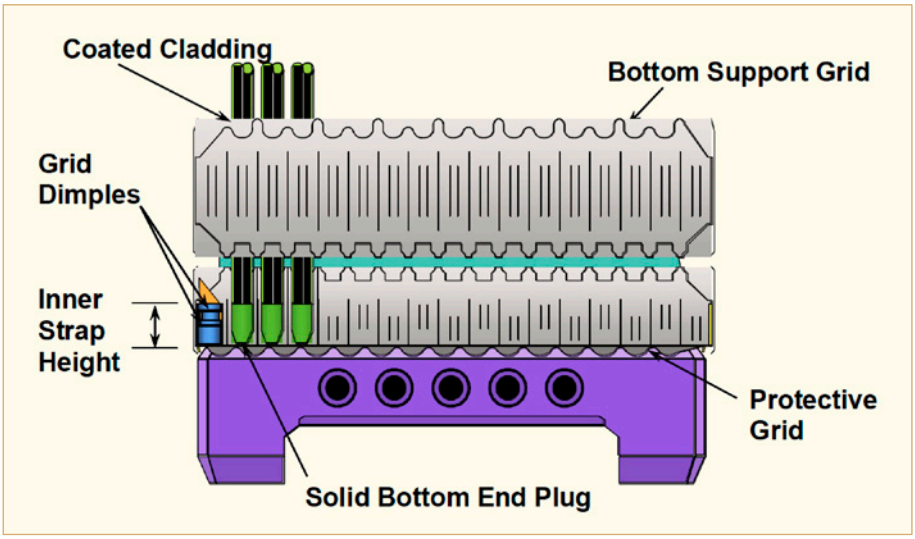

Figure 2-7: Multiple levels of debris protection on the Westinghouse-type fuel designs [Bradfute et al, 2012].

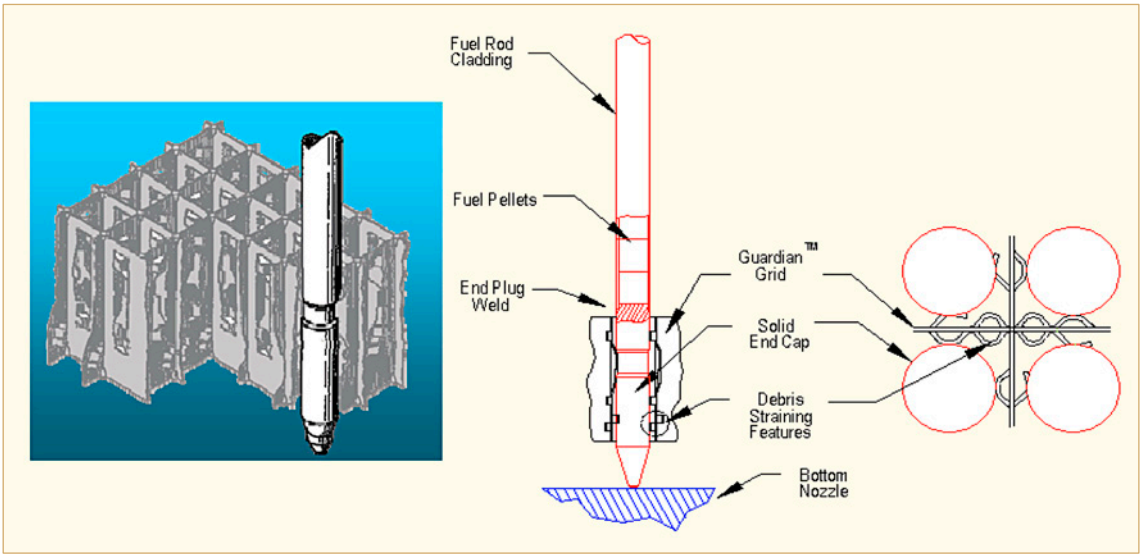

Figure 2-8: Guardian grid used in the CE 16x16 NGF design [Bradfute et al, 2012].

The RFA design is described in the paper by [Aulló et al, 2012]. The features of the RFA design include (Figure 2-9):

- Removable top nozzle
- DFBN
- Inconel 718 top grid
- Structural RFA-2 mid grids
- Inconel 718 bottom grid
- Inconel 718 protective bottom grid
- Thicker thimble tubes
- Tube-in-tube dashpot

To reduce fuel assembly bow the skeleton stiffness was increased by increasing the guide thimble and instrument tube wall thickness with 25% relative to the previous design. Also, using the ZIRLO material in the guide thimbles (not incorporated in the first designs for EDF) reduces bow due to lower irradiation growth rate and creep [Aulló et al, 2012] (Figure 2-10).

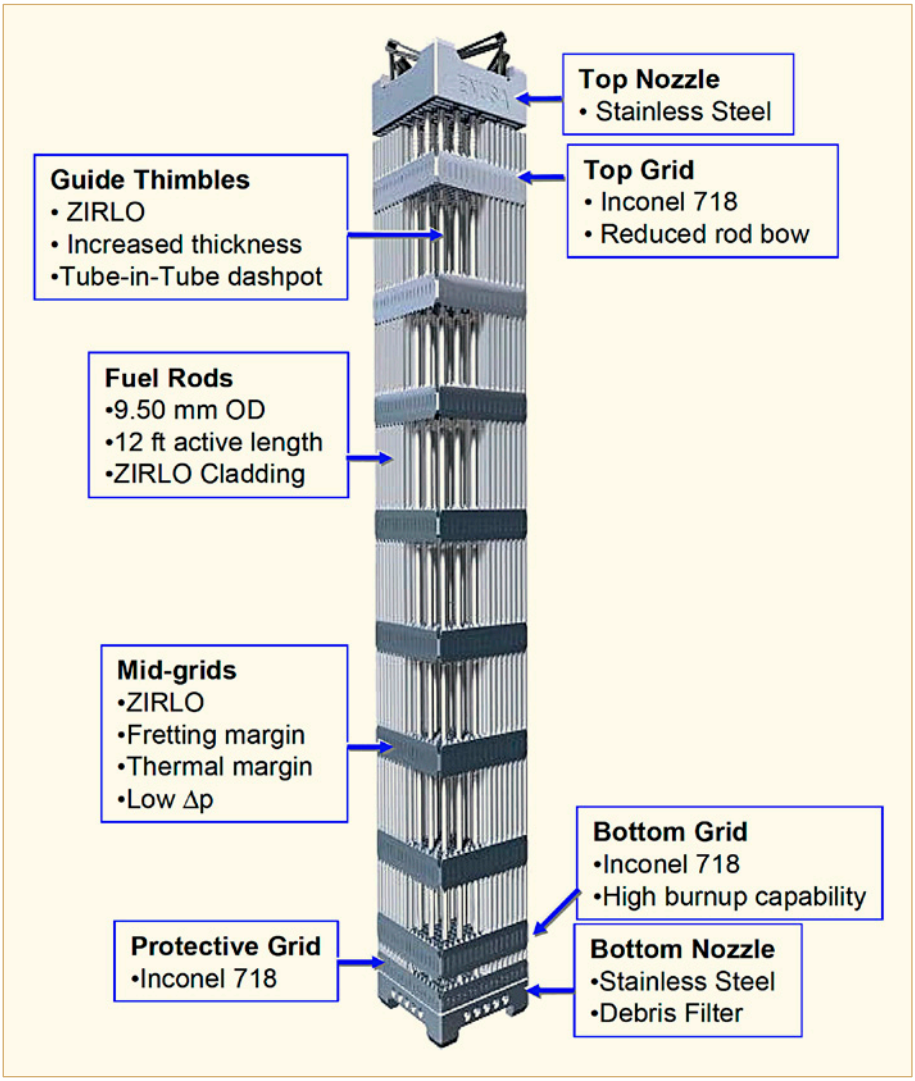

Figure 2-9: RFA fuel [Aulló et al, 2012].

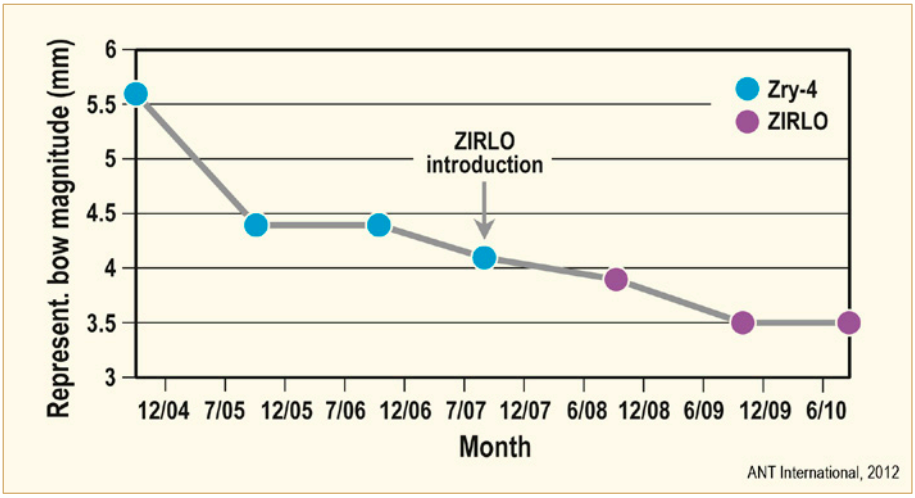

Figure 2-10: Bow evolution in Gravelines 6 (RFA 900 and RFA 900 ZIRLO), after [Aulló et al, 2012].

2.4.2 AREVA

2.4.2.1 BWR

The ATRIUM 11 is AREVA's latest fuel design with the following characteristics [Garner, 2012], [Cole et al, 2012]:

- The 11x11 lattice provides a fully symmetric array of 112 fuel rod positions vs. the 91 to 96 rods in the previous 10x10 design (Figure 2-11):
  - The total fuel column length within the bundle is increased ~20% over AREVA's ATRIUM™ 10XM design. This increase reduces the linear heat generation rate (LHGR) of the individual fuel rods for a given bundle power.
- The 3rd Generation FUELGUARD filter (no line of sight) is able to filter straight wires with a diameter of > 0.2 mm and a length of > 8 mm with nearly 100% efficiency. In addition, the filter is able to prevent thinner flexible wires from entering the filter with help from special features (twists) at the filter's entrance plane [Blavius et al, 2012] (Figure 2-12).
- The modular Upper Tie Plate (UTP) with Double Strip Grid (DSG) was developed to avoid debris with a diameter > 7 mm from entering the fuel assembly from the top (the corresponding debris size for ATRIUM 10XM > 18 mm) [Blavius et al, 2012] (Figure 2-12).
- The monometallic ULTRAFLOW spacer with a debris rejecting strip shape and debris capture resistant rod bearing elements (springs/dimples) (Figure 2-12) [Blavius et al, 2012].
- Cr_2O_3 doped fuel pellets in non-liner cladding (Cr_2O_3 doped fuel is nearing the end of an independent development programme according to the authors) to lower FGR (targeting a matrix grain size of 50 to 60 µm obtained with an optimum Cr_2O_3 amount of 0.16 wt.%) and increase the PCI margin.

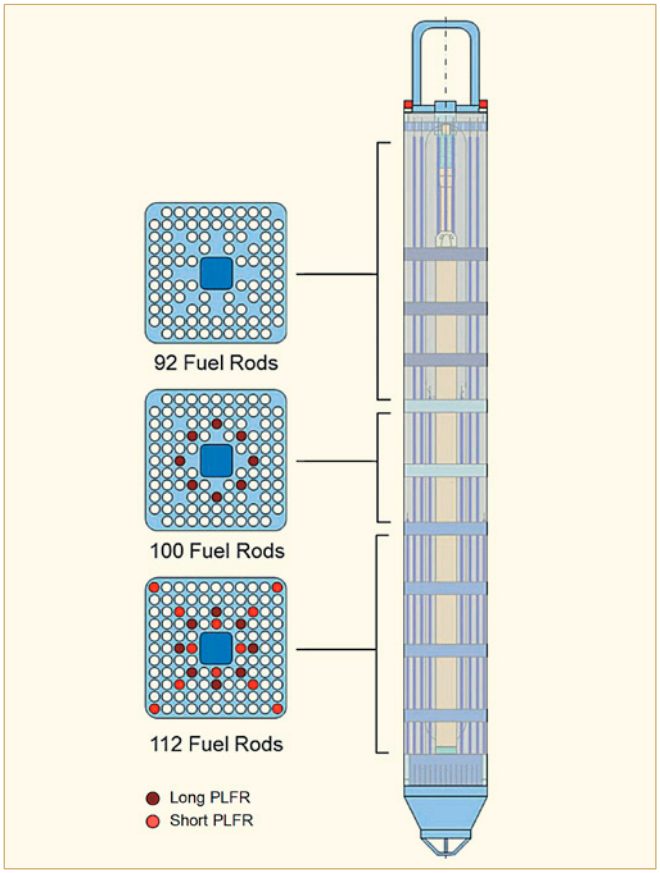

Figure 2-11: Axial and radial configuration of the ATRIUM 11 [Garner, 2012].

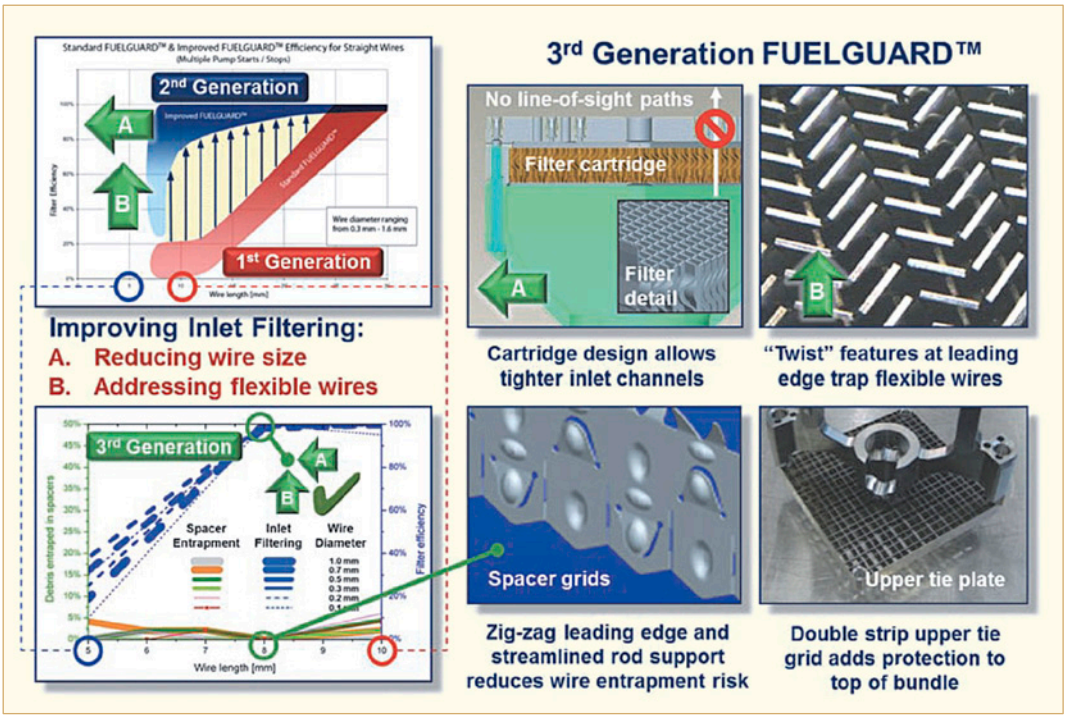

Figure 2-12: The 3rd generation FUELGUARD debris filter reduces the length of wire able to pass into the fuel rod array by ~33%. Leading edge "twist" features were shown in testing to capture and hold flexible debris, blocking further progress into the bundle while preventing release during fuel handling [Garner, 2012].

2.4.2.2 PWR

Two AREVA PWR fuel technologies are used for EPR reactors as reference fuel for licensing and first cores (Table 2-3) [Gentet et al, 2012].

Table 2-3: Main features of EPR first cores fuel, after [Gentet et al, 2012].

	HTP LE	AFA 3G LE
Bottom nozzle	Robust FUELGARD	TRAPPER
Fuel rods	265 M5-clad fuel rods	265 M5-clad fuel rods
Bottom end grid/Top end grid	Alloy 718 HMP/Alloy 718 HMP	AFA 3G twin-grid/AFA 3G grid
Mixer spacers	8 M5-HTP	8 M5-AFA 3G
Guide tubes	24 M5-MONOBLOC	24 M5-MONOBLOC
Upper connection	24 Quick-disconnect connections	24 Quick-disconnect connections
		ANT International, 2012

The EPR development was based on the latest PWR product lines N4 and Konvoi, of former Framatome and Siemens respectively (Table 2-4).

Table 2-4: Core characteristics, after [Gentet et al, 2012].

Type of power plant	EPR™	N4	Konvoi
Thermal power (MW)	4250 to 4900	4250	3850
Number of FA	241	205	193
Number of absorber rods	89	73	61
Fissile height (cm)	420	427	390
Number of fuel rod per assembly	265	264	300
Average linear power (W/cm)	155 to 179	180	167
			ANT International, 2012

The main differences of EPR fuel design, compared to existing 17x17- 14ft designs are:

- The fuel assembly consists of 265 fuel rods with a lower plenum and, the instrumentation system is introduced from the top of the fuel assembly (hence the instrumentation tube is eliminated and the top nozzle modified).
- The bottom nozzle height is the same as for the 12-foot fuel assemblies although it is a 14ft design. This change allows more space for the fuel rod and the fission gas plenum – thus more margins towards lift-off.
- The fissile fuel height is reduced by 70 mm while the total rod length is slightly increased.

5 Dimension stability

5.1 Irradiation growth of zirconium alloys (Ron Adamson)

5.1.1 Introduction

One of the most unique aspects of material behaviour in a nuclear power plant is the components. In fast breeder reactors the Fe and Ni-based alloys creep and swell, that is, they change dimensions in response to a stress and change their volume in response to radiation damage. In light water reactors, zirconium alloy structural components creep, do not swell, but do change their dimensions through the approximately constant volume process called irradiation growth. Radiation effects are not unexpected since during the lifetime of a typical component every atom is displaced from its normal lattice position at least 20 times. With very few exceptions, the mechanical and physical properties needed for reliable fuel assembly performance are affected by irradiation. A summary of such effects is given by [Adamson, 2000].

Practical effects of dimensional instabilities are well known and it is a rare technical conference in the reactor performance field that does not include discussions on the topic. In addition to lengthening due to irradiation growth, many components are subjected to creep stresses. Because of the difference in pressure inside and outside the fuel rod, cladding creeps down on the fuel early in life, and then creeps out again later in life as the fuel begins to swell. A major issue is to have creep strength sufficient to resist outward movement of the cladding if fission gas pressure becomes high at high burnups. PWR guide tubes can creep downward or laterally due to forces imposed by fuel assembly hold down forces or cross flow hydraulic forces – both leading to assembly bow which can interfere with smooth control rod motion. BWR channels can creep out or budge in response to differential water pressures across the channel wall, again leading toward control blade interference. Fuel rods, water rods or boxes, guide tubes, and tie rods all can lengthen due to irradiation growth, possibly leading to bowing problems. (For calibration, a recrystallised (RX or RXA) Zircaloy water rod or guide tube could lengthen due to irradiation growth more than 2 cm. during service; a cold worked/stress relieved (SRA) component could lengthen more than 6 cm.) Even RX spacer/grids could widen enough due to irradiation growth (if texture or heat treatment was not optimized) to cause uncomfortable interference with the channel.

In addition, corrosion leading to hydrogen absorption in Zircaloy can contribute to component dimensional instability due, at least in part, to the fact that the volume of zirconium hydride is about 16% larger than zirconium.

The above discussion leads to the concept that understanding the empirical details and mechanisms of dimensional instability in the aggressive environment of the nuclear core is important for very practical reasons. Reliability of materials and structure performance can depend on such understanding.

A comprehensive review of dimensional stability has been given in the ZIRAT7/IZNA2 Special Topical Report (STR) [Adamson & Rudling, 2002/2003], ZIRAT10/IZNA5 STR [Adamson & Cox, 2005/2006], ZIRAT10/IZNA5 STR [Cox et al, 2005/2006], ZIRAT14/IZNA9 STR [Adamson et al, 2009a], and ZIRAT16/IZNA11 STR [Garzarolli et al, 2011].

The sources of dimensional changes of reactor components (in addition to changes caused by conventional thermal expansion and contraction) are: irradiation growth, irradiation creep, thermal creep, stress relaxation (which is a combination of thermal and irradiation creep), and hydrogen and hydride formation.

Irradiation effects are primarily related to the flow of irradiation-produced point defects to sinks such as grain boundaries, deformation-produced dislocations, irradiation-produced dislocation loops, and alloying and impurity element complexes. In zirconium alloys, crystallographic and diffusional anisotropy are key elements in producing dimensional changes.

In the past, hydrogen effects have been considered to be additive to and independent of irradiation; however, recent data have brought this assumption into question. It is certain that corrosion-produced hydrogen does cause significant dimensional changes simply due to the 16-17% difference in density between zirconium hydride and zirconium. A length change of on the order of 0.25% can be induced by 1000 ppm hydrogen in an unirradiated material. Whether or not the presence of hydrogen and/or hydrides contributes to the mechanisms of irradiation creep and growth is yet to be determined.

Fuel rod diametral changes are caused by stress dependent creep processes, as irradiation growth in the hoop direction is very small.

Fuel rod length changes are caused by several phenomena:

- Stress free axial elongation due to irradiation growth.
- Anisotropic creep (before pellet/cladding contact) due to external reactor system pressure. Because of the tubing texture, axial elongation results from creep down of the cladding diameter; however for heavily cold worked material, it has been reported that some shrinkage may occur. In a non-textured material such as stainless steel, creep down of the cladding would only result in an increase in cladding thickness, with no change in length (more detail below).
- Creep due to pellet-cladding mechanical interaction (*PCMI*) after hard contact between the cladding and fuel. This occurs in mid-life, depending on the cladding creep properties and the stability of the fuel.
- Hydriding of the cladding due to corrosion.

Bow of a component such as a BWR channel or PWR control rod assembly can occur if one side of the component changes length more than the other side. Such differential length changes occur due to differential stress and creep, to relaxation of differential residual stresses, or to differential growth due to differences in flux-induced fluence, texture, material cold work, and hydrogen content (and, although not usually present, differences in temperature or alloying content), ZIRAT16/IZNA11 STR [Garzarolli et al, 2011].

The texture in (anisotropic) Zr alloys can cause an axial length change due to anisotropic in-reactor creep under a 2 to 1 tangential to axial stress ratio, as arises under a pressure difference (between system and rod internal pressure), before pellet-cladding contact, and some Pellet Cladding Mechanical Interactions (PCMIs) on components such as pressure tubes or fuel rod claddings.

In an isotropic material such as stainless steel, internally pressurized closed end tubing undergoes no length change (just a diameter increase and a wall thickness decrease). However in anisotropic Zr-alloys with textures typical of fuel rod tubing, internal pressure causes a decrease in length for RXA (recrystallised) material and an increase in length in CW or SRA (stress relieved) material. If the sign of the hoop stress is reversed, the respective length changes are reversed. Figure 5-1 gives some representative data, Garzarolli in [Adamson et al, 2009a]. The data used to calculate the anisotropy factors (ratio of axial to hoop strain) is presented by [Gilbon et al, 2000] and [Soniak et al, 2002].

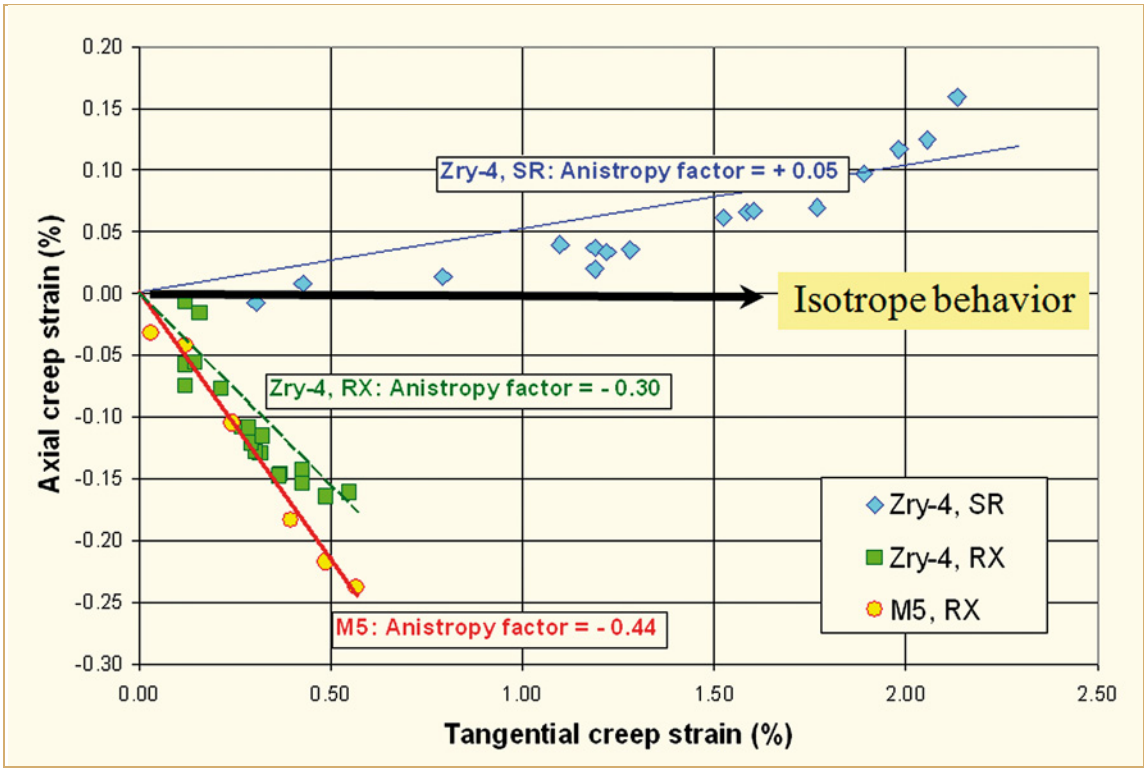

Figure 5-1: In-reactor creep of closed-end tubes with 2-1 ratio of hoop to axial stress. Note that the above tests were performed on tubes with an internal overpressure which results in outward creep (contrary to what happens in a reactor). The above figure shows that tube creep out (indicated by a positive tangential creep strain) shortening of Zircaloy-4 and M5 RXA tubes while a small elongation of the Zry-4 SRA tube. The above data are also valid for in-pile fuel rods but in this case, the fuel clad creep down would result in elongation of RXA tubes while a small shortening of SRA tubes. Data extracted from [Gilbon et al, 2000] and [Soniak et al, 2002].

In-reactor dimensional stability (or in-stability!) affects the dimensions of all Zirconium-alloy components during exposure in the core of reactors. Important components and their environmental conditions include:

- The pressure tubes of CANDU and RBMK reactors that contain the fuel assemblies (FAs). CANDU pressure tubes have a particular (tangential) texture and microstructure governed by ß-quenching, extrusion, and drawing. They operate at temperatures between 250-310°C under a fast flux of 0.5-3.E13 n/cm².s (>1 MeV) and are stressed by the coolant pressure on the inside to a hoop stress of about 100 MPa. Target design life is 30 years at 80% capacity. For RBMK pressure tubes, the design lifetime is considerably shorter, on the order of 20 years.

- The thin wall fuel rod (FR) claddings of PWR/VVER and BWR have a radial texture governed mostly by the last rocking steps, and a medium GS affected by intermediate annealing and cold deformation. Fuel rods are stressed by the coolant overpressure at the beginning of irradiation (compressive hoop stress of 40-80 MPa) and eventually by fuel swelling at the end of life (tensile hoop stress up to >50 MPa in SR PWR fuel rods and up to >100 MPa in Recrystallised (RXA) BWR fuel rods) and are exposed to a fast neutron flux of 0.2-2x10^{14} n/cm².s. The fuel cladding can in addition, in case of fast power uprates, experience as a consequence of Pellet Cladding Interaction (PCI) rather high tensile stresses (>500 MPa) that relax quickly by in-reactor creep. The cladding outer-surface temperature is in case of BWR claddings about 290°C and is significantly higher in case of PWR claddings, 320-360°C. Max exposure times are up to 10 years for BWR fuel and up to 6 years for PWR fuel.

- The guide tubes (GT) of PWR/ VVER fuel assemblies (FAs) with a similar texture and structure as the fuel rods provide together with the spacers the major structural support. However, large friction forces between the grid and fuel rods may provide some additional structural support from the fuel rods. The GT also provide the path for moving control rod cluster. The GTs are loaded axially by the hold down spring force, the hydraulic forces, the differential expansion of fuel rods and GTs and by bow forces from cross flow and neighbouring FAs. The actual forces depend on the frictional connection via the spacers between GTs and FRs and may be between several 10 MPa compressive up to several 10 MPa tensile. In addition, the GT growing oxide layer may create axial tensile stresses up to about 10 MPa. The square BWR flow channel is the main structural component of a BWR fuel element, providing adequate stiffness and is the main load bearing structure during seismic events and accident conditions. It also provides a cruciform path for control blade manoeuvring. They are stressed by the difference between the coolant pressure and the pressure in the outer bypass region, which increases with increasing height. They are made from strips, with the typical strip texture. Maximum stress arises at the corner (several 10 MPa tangential stress). In-reactor creep at this position results in bulging.

Irradiation growth occurs simultaneously with irradiation creep if there is an applied stress. The two processes are considered to be independent and additive, even though they compete for the same irradiation-produced defects mechanistically. When assessing dimensional changes of any component all sources of change must be taken into account. This is especially true for fuel rods, which will invariably have length-change components due to irradiation growth and anisotropic creep, and perhaps pellet-imposed stresses at higher burnups.

In this Annual Report (AR) review aimed at irradiation growth, we will primarily address conditions of direct interest to LWRs and CANDUs, unless the information has mechanistic implications. Specific issues mentioned above will be addressed separately below.

5.1.2 Basics of irradiation growth

Irradiation growth is a change in the dimensions of a zirconium alloy reactor component even though the applied stress is nominally zero. It is approximately a constant volume process, so if there is, for example, an increase in the length of a component, the width and/or thickness must decrease to maintain constant volume. Understanding of the detailed mechanism is still evolving; however a clear correlation of growth to microstructure evolution exists, and many empirical observations have revealed key mechanistic aspects. The inherent anisotropy of the Zr crystallographic structure plays a strong role in the mechanism, as materials with isotropic crystallographic structure (like stainless steel, copper, Inconel, etc.) do not undergo irradiation growth. It is not to be confused with irradiation swelling, which does conserve volume and does not occur in zirconium alloys under normal reactor operating conditions.

Irradiation growth is strongly affected by fluence, cold work, texture, irradiation temperature, and material chemistry (alloying and impurity elements), as will be described in later sections. Figure 5-2 gives schematic growth curves illustrating several points. Note that L-textured material (blue) grows, while T-textured material (red) shrinks; when taken with the third direction (N) in a component, this behaviour results in approximately constant volume. The long direction (L) of a component is the most important; for instance the length of a fuel rod, channel box or guide tube. Note that cold worked (CW) material grows at a high and almost linear rate, while recrystallised (RXA) material grows in a 3-stage process, with the final high rate being called “breakaway” growth. The various stages can be directly related to the irradiation-produced microstructure, described, example in [Adamson, 2000] Section 1.2 [Rudling et al, 2007]. For RXA Zircaloy, at low fluences where only <a> component loops exist, growth is small (~0.1%) and saturates. When <c> component loops begin to appear the growth rate increases and becomes nearly linear with fluence in the range 6-10 x 10^{25} n/m^2, E > 1 MeV (1-2 dpa, 30-50 GWd/Mt). For L-texture material growth can reach 1% at 20 x 10^{25} n/m^2 (30 dpa; 100 GWd/Mt burnup) in initially cold worked (CW) or cold worked

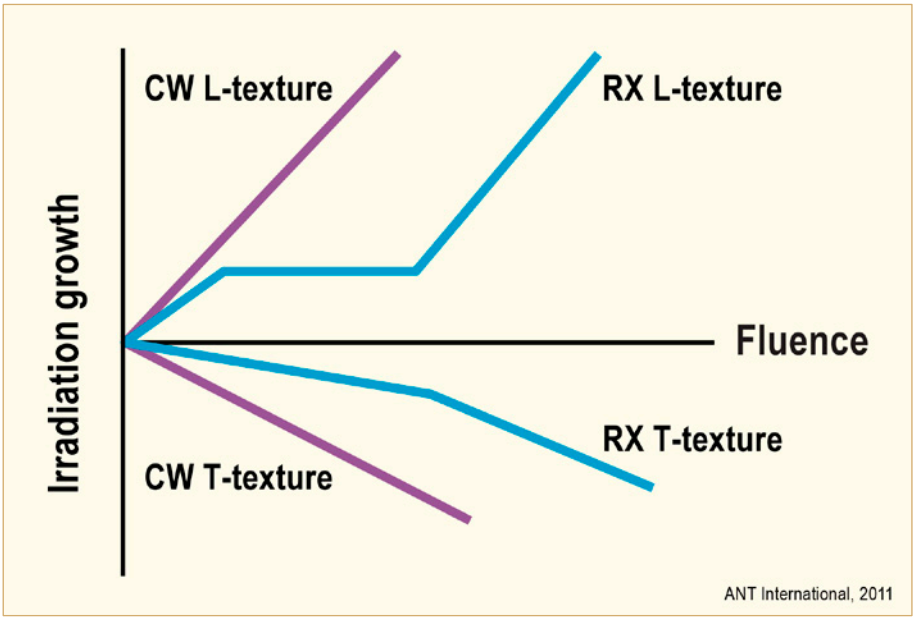

Figure 5-2: Schematic curves for irradiation growth as a function of fluence for recrystallised (RXA) and cold worked (CW) Zircaloy having textures characterized as L (f ≈ 0.1) and T (f ≈ 0.4) and an irradiation temperature near 300°C (573K).

stress relieved material (SRA), <c> component dislocations occur as part of the deformation-induced structure and more are formed during irradiation [Holt et al, 1996]. The growth rate is nearly linear with fluence and the magnitude is almost linear with the amount of initial cold work. In heavily-worked material (typically 70 – 80% in a fuel rod) a growth of 2% can be reached by 20 x 10^{25} n/m^2. An overview of factors affecting growth is given by [Fidleris et al, 1987].

Irradiation growth has a linear dependence on fast flux [Holt, 2008]. Therefore growth can be plotted against fast fluence (flux x time), as is commonly done, without regard for the value of flux.

The key practical, empirical mechanistic feature of irradiation growth is the presence of <c> component dislocations (either as irradiation-produced loops or deformation-induced networks). Without them "breakaway" growth does not occur. This is illustrated in Figure 5-3 for CW or RX Zircaloy irradiated at low (80°C (353K)) or intermediate (553K (280°C)) temperature, [Rogerson, 1988a]. For all four conditions (A, B, C, D) a high density of <a> loops forms early in life and saturates at <20x10^{24} n/m^2. The loops at 553K (280°C) are larger than at 353K (80°C), which may account for the difference in growth magnitudes for conditions C(red) and D(green), but the effect is minor. For condition D (353K) to high fluence or condition C (553K) to less than <40x10^{24} n/m^2 there are no <c> component dislocations observed in the microstructure and growth is low.

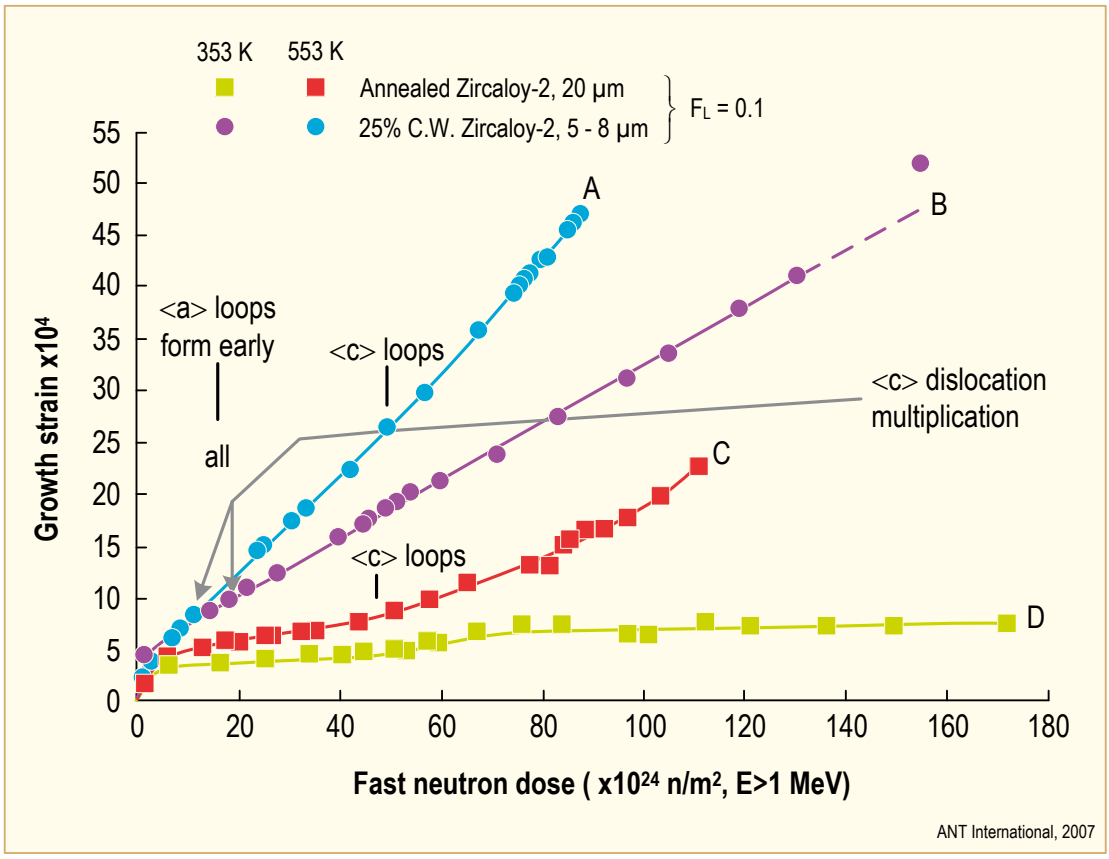

Figure 5-3: Irradiation growth in annealed and 25% cold-worked Zircaloy-2 at 353 and 553 K, after [Rogerson, 1988a].

In condition C (553K (280°C)), <c> loops begin forming at about 40x10^{24} n/m^2, at which point the growth of conditions C and D become different. No <c> loops are observed in condition D (353K (80°C)) out to high fluence [Griffiths et al, 1996].

For conditions A(blue) (553K (280°C)) and B(purple) (353K (80°C)), net works containing <c> component dislocations induced by cold work exist before irradiation, and the <c> components multiply during irradiation (by a process of helical climb with loops spreading out on the basal plane [Holt et al, 1996]. In addition, condition A (at 553K) is expected to form irradiation-induced <c> loops [Griffiths et al, 1996].

The experimental measurement of increase in <c> component density as a function of fluence is shown in Figure 5-4, and the saturation of <a> loop density with fluence is shown in the upper two curves (Figure 5-5). The measurement of <c> loop density can also be done by transmission electron microscopy (TEM); however the measurement technique has many difficulties induced by the large size of the loops relative to the thickness of the TEM foil and the problems of firmly identifying loops. Figure 5-6 gives a estimate of loop density measured all by the same technique, [Mahmood et al, 2000].

It can be concluded that high growth rates can be correlated to the existence of <c> component dislocation loops and defects.

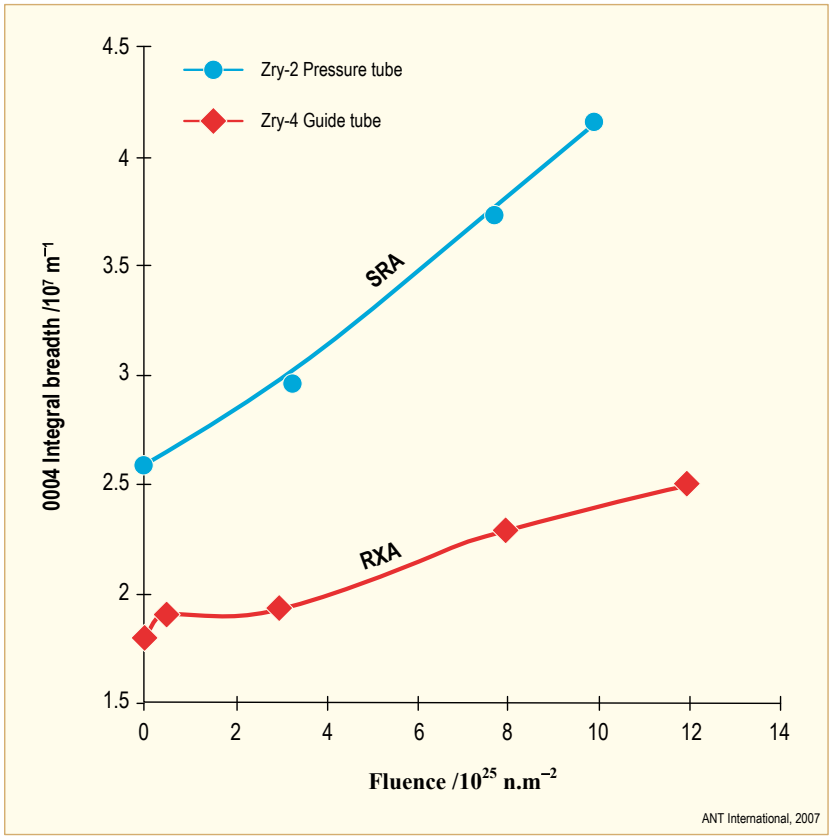

Figure 5-4: Variation in basal line broadening as a function of neutron fluence at about 570 K for annealed Zircaloy-4 guide tubes and cold-worked Zircaloy-2 pressure tubes using RN(1120), after [Griffiths et al, 1996].

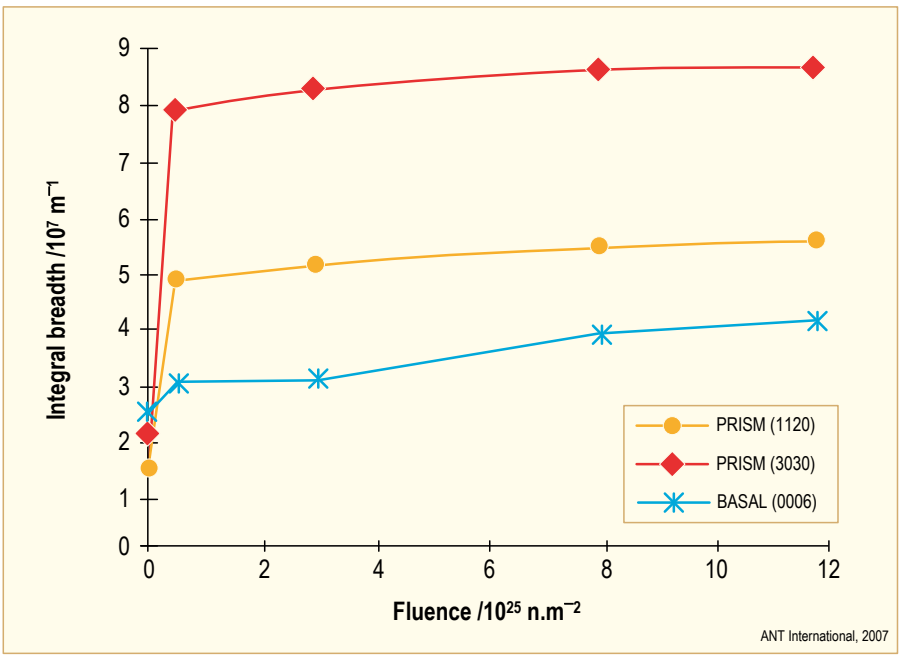

Figure 5-5: Variation in integral breadths as a function of neutron fluence for Zircaloy-4 guide tubes irradiated at 560 to 580 K using RN(1120), LN(2020), and TN(0004) specimens cut perpendicular to the radial, longitudinal, and transverse axes of the tube, respectively, after [Griffiths et al, 1996].

6 Out-of-pile and in-pile corrosion & hydriding (Friedrich Garzarolli)

6.1 PWR fuel rod corrosion analysis

Exposure of lead test assemblies (LTA) is necessary if:

- A new cladding material is being developed,
- a more demanding fuel cycle is planned, or
- a new water chemistry, that may affect corrosion, shall be introduced.

The examination of such LTA certainly should include fuel rod oxide thickness measurements. A reliable analysis of the observed fuel rod oxide thickness values is necessary to confirm that fuel rod corrosion remains acceptable. In principle 4 different possibilities exist for the analysis:

a) A graph showing the peak oxide thickness values versus the fuel rod burnup,

b) a graph showing the peak oxide thickness versus an index considering exposure time and fuel duty, e.g. the Modified Fuel Duty Index of Westinghouse [Kesterson et al, 2006],

c) an estimation of the in PWR fuel rod corrosion via an computer model, e.g. the EPRI PWR fuel rod corrosion model [Cheng et al, 1996], or

d) a detailed data analysis via the normalized time, as proposed in the [Garzarolli et al, 2012].

Method (a) can be used for a comparison of different alloys under comparable fuel duty, as shown in Figure 6-1. However, the burnup dependency is strongly governed by the fuel duty, as shown in Figure 6-2 for Zircaloy-4, which behaves very different in different PWRs with a different fuel duty.

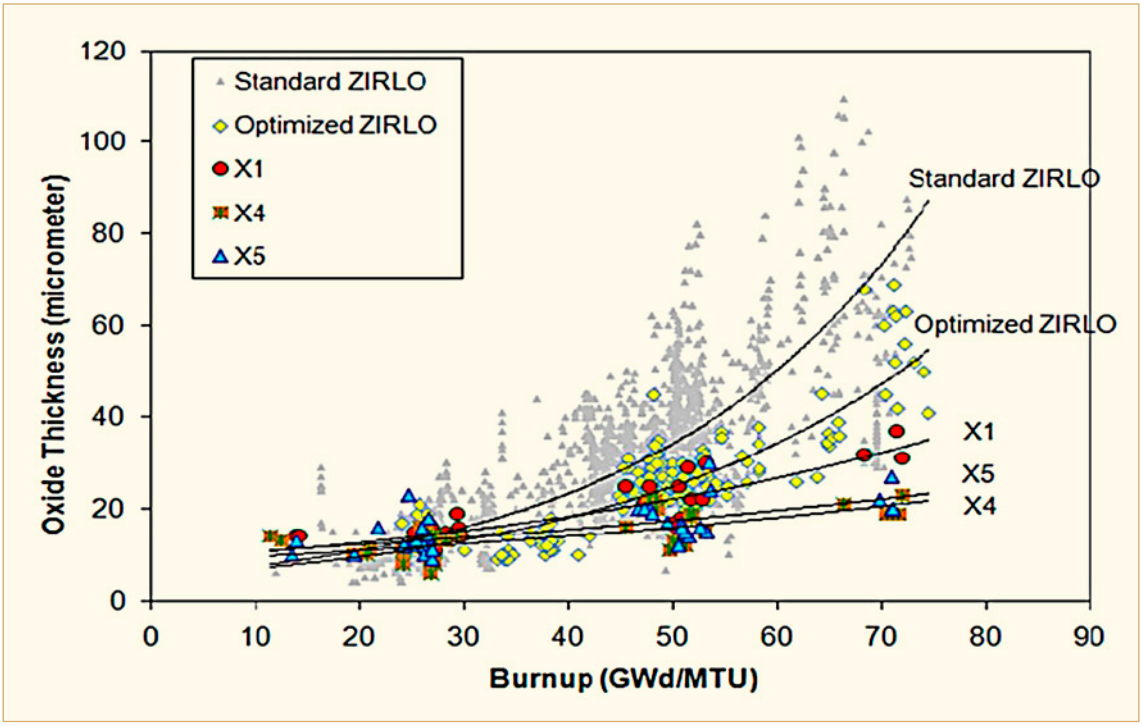

Figure 6-1: Corrosion of ZIRLO, Optimized ZIRLO and AXIOM Alloys X1, X4 and X5 [Foster et al, 2011].

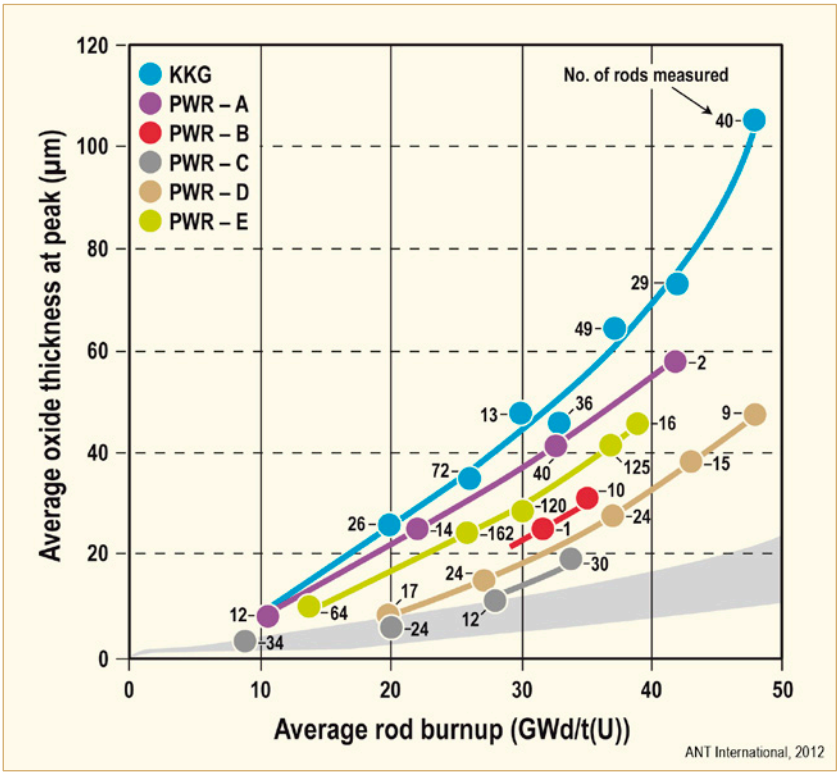

Figure 6-2: Peak oxide thickness of Zry-4 fuel rods versus burnup from different PWRs and comparison with predicted values assuming no irradiation corrosion enhancement, after [Garzarolli et al, 1985].

Method (b) using an index, that considers exposure time and fuel duty, such as the Modified Fuel Duty Index of Westinghouse (Figure 6-3), allows certainly a better transferability to other fuel duties, however it does not consider the feedback effect of the oxide layer itself and does not allow to evaluate particular corrosion characteristics.

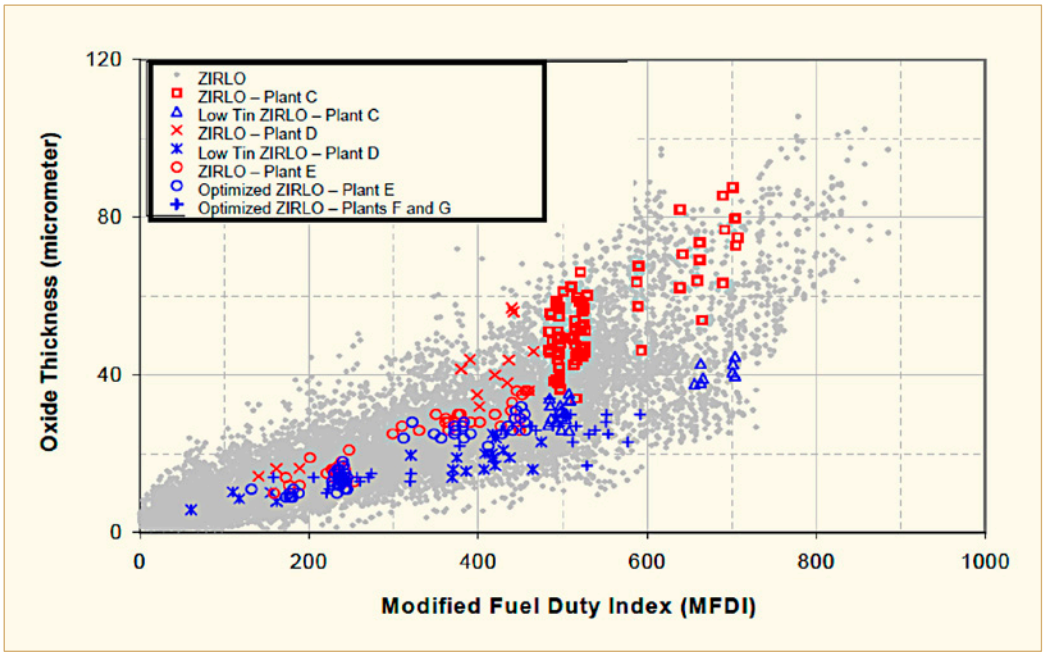

Figure 6-3: Oxide thickness vs., Modified Fuel Duty index (MFDI) for ZIRLO, Low Tin ZIRLO and Optimized ZIRLO [Wikmark et al, 2008].

Method (c) needs every time an elaborate study and program development, to analyze particular aspects.

Method (d) is the only method that leads with little effort to reasonable conclusions, which can be easily transferred for future application, as will be shown in the following.

For final conclusions it is very important to evaluate the corrosion behaviour for all possible effects, such as:

- Normal corrosion behaviour of a particular Zr alloy and material condition
- Corrosion enhancement due to SPP dissolution, above a certain burnup dependent on temperature
- Temperature independent corrosion enhancement at high burnup
- Hydride rim induced corrosion enhancement
- Corrosion effects due to steaming as proposed by [Kesterson et al, 2006]
- Li induced corrosion effects

All this phenomena are discussed in detail in [Garzarolli et al, 2012]. The report contains also a program to calculate for a particular fuel rod examined for its oxide thickness the local oxide metal temperature, the local steaming rate, the local normalized time or enhancement factor versus the Zry-4 out reactor (Matthias-I) and a second for predicting the oxide profile for a fuel rod with the same cladding under a different fuel duty (Matthias-II).

In the following, applying this model, some conclusions are shown that are important to consider.

Often only the peak oxide thickness at the outer periphery of fuel rods is measured. Such measurements on the outer periphery, however, suffer from the fact that the gap to the neighbouring FAs at spacer positions, which is nominally about 2 mm, could be increased or decreased by FA bow. To check the consequence of such a FA bow induced gap variations on the peak oxide thickness, calculations were made applying the program Matthias-II. For this calculations the average power history of the ZIRLO rods exposed in Vandellos II, as reported by [Tsukuda et al, 2003] and [Watanabe et al, 2005] were performed and compared with the reported data (Figure 6-4). The figure reveals that the oxide thickness would be about 20-70% (increasing with oxide thickness respectively burnup) higher if the gap size is reduced by 2 mm and about 17% lower if the gap size increased by 2 mm. This means that conclusions based on such measurements have quite large uncertainties. Fully reliable conclusions can only be drawn from internal rods.

7 Primary failure and secondary degradation – open literature data (Peter Rudling)

The open literature data are provided in the following sections.

7.1 Introduction

7.1.1 Primary failures

During reactor operation, the FR may fail due to a primary cause such as fretting, PCI manufacturing defects, corrosion, etc. (Table 7-1).

Table 7-1: Primary failure causes for LWR fuel during normal operation and Anticipated Operational Occurrences (AOO).

Primary failure cause	Short description
Excessive corrosion	An accelerated corrosion process results in cladding perforation. This corrosion acceleration can be generated by e.g., CRUD deposition (CILC[38]), Enhanced Spacer Shadow Corrosion, (ESSC),[39] (in BWRs), dry-out due to excessive FR bowing.
Manufacturing defects	Non-through-wall cracks in the fuel cladding developed during the cladding manufacturing process. Defects in bottom and/or top end plug welds. Primary hydriding due to moisture in fuel pellets and or contamination of clad inner surface by moister or organics. Too large a gap between the FR and the spacer grid supports (poor spacer grid manufacturing process) leading to excessive vibrations in PWR fuel causing fretting failures. Chipped pellets may result in PCI failures both in liner and non-liner fuel.
PCI	PCI—an iodine assisted SCC phenomenon that may result in fuel failures during rapid power increases in a FR. There are three components that must occur simultaneously to induce PCI and they are: 1) tensile stresses—induced by the power ramp, 2) access to freshly released iodine-occurs during the power ramp, provided that the fuel pellet temperature becomes large enough and 3) a sensitised material—Zircaloy is normally sensitive enough for iodine stress-corrosion cracking even in an unirradiated state.
Cladding collapse	This failure mechanism occurred due to pellet densification. This failure mode has today been eliminated by fuel design changes and improved manufacturing control.
Fretting	This failure mode has occurred due to: Debris fretting in BWR and PWR. Grid-rod fretting - Excessive vibrations in the PWR FR causing fuel failures. This situation may occur for example due to different pressure drops in adjacent FAs causing cross-flow. Baffle jetting failures - Related to unexpectedly high coolant cross-flows close to baffle joints.
	ANT International, 2012

[38] CILC – an accelerated form of corrosion that has historically resulted in a large number of failures in BWRs. Three parameters are involved in this corrosion phenomenon, namely: 1) Large Cu coolant concentrations as a result of e.g., aluminium brass condenser tubes, 2) Low initial fuel rod surface heat flux – occurs in Gd rods and 3) Fuel cladding that shows large initial corrosion rates- occurs in cladding with low resistance towards nodular corrosion.

[39] This corrosion phenomenon resulted recently in a few failed rods. The mechanism is not clear but seems to be related to galvanic corrosion. This corrosion type may occur on the fuel cladding in contact or adjacent to a dissimilar material such as Inconel. Thus, this accelerated type of corrosion occurred on the fuel cladding material at spacer locations (the spacer springs in alloy BWR fuel vendors fuel are made of Inconel). Water chemistry seems also to play a role if the fuel cladding material microstructure is such that the corrosion performance is poor. Specifically coolant chemistry with low Fe/(Ni-Zn) ratio seems to be aggressive (provided that the cladding material shows poor corrosion performance. A fuel cladding material with good corrosion resistance does not result in *ESSC*, even in aggressive water chemistry.

Table 7-2 and Table 7-3 provide key data for some of the most recent fuel-failure cases.

Table 7-2: Summary of previous PWR failure key events, see previous ZIRAT/IZNA-reports for details.

Nuclear unit	Type of primary failure	Comment
TMI-1, Cy 10, 1995	Nine high peaking FRs, Zr-4 Cladding, failed after 122 days of operation. CRUD/corrosion related failures.	All failed and degraded pins reportedly had Distinctive CRUD Pattern (DCP)[40]. High peaking factors, thermal-hydraulic conditions. Calculations indicated that no boiling should have occurred on the pins with DCP, although the pins with DCP were calculated to have a slightly higher temperature. Water chemistry (low pH at BOC, pH < 6.9, max LiOH 2.2 ppm). Some, AOA effect was found reaching a maximum in the middle of cycle 10. The source of the CRUD could not be determined. The CRUD sampling showed that the nickel-to iron ratio was in the range 1.25 to 16.7, which was reportedly somewhat lower than in previous investigations.
Seabrook, Cy 5, 1997	Five one-cycle ZIRLO rods failed. CRUD/corrosion related failures.	Longer cycle in transition to 24-month cycle. Possibly CRUD-induced overheating resulting in substantial nucleate boiling.
EdF data reported in 2009 [Thibault et al, 2009	The main failure causes in the EdF plants are: GTRF wear, Clad manufacturing defects and, Excessive fuel assembly bowing (resulting in assemblies grids hanging-up during loading and unloading and IRI)	A significant number of fuel failures were related to the M5 fuel cladding in 1300 MWe and 1450 MWe units. The M5 FR failures were due to fabrication defects either related to the end plug girth or fill hole weld or defects in the fuel clad itself at grid levels (related to the pulling of the rods into the assembly structure). To resolve these manufacturing issues, AREVA has modified the welding techniques as well as the rod pulling procedure. It was observed that there were no GTRF failures in 2008 (in previous years there have always been some GTRF failures). The reasons for the great improvement is thought to be due to that both AREVA and Westinghouse have introduction reinforced FAs design (AFA3GLr – AREVA and RFA2-Westinghouse). Since the introduction of the AREVA AFA3G design in 1999, a decrease of the average core bow in EdF NPPs has been observed, especially on the 900 MW units, but not as fast as expected. The maximum values of bowing remain relatively high on the 1300 MW units, typically between 15 and 19 mm for a “S shape” bow. The Westinghouse RFA fuel design behaves in the same way with similar bowing range while HTP assembly deformations are twice less. Incomplete Rod Insertions (IRIs) due to bowing have been significantly reduced since the AFA3G FA’s design has been loaded in EdF NPPs and despite the increasing of the average discharge burn-up of the FAs. In 2008, no anomaly of RCCA drop time was observed in EdF NPPs during the BOC tests. Concerning the EOC tests, no anomaly was observed in the 12 feet units whereas four RCCAs dropped without recoil in the 14 feet units. Three of them was AFA3G FAs (two “2nd cycle” FAs and one “4th cycle” FA) and one was the older design (AFA2G). The number of FAs damaged during handling operations has decreased in 2008 but remains significant. The damages concern only AFA 2G or 3G design and mainly the 14 feet units. It occurs during the unloading operations. The damages generally occur during a “three-sided box” extraction and result from grids’ hanging due to bowing and to a reduced gap between FAs following unexpected grid growth due to re-crystallized Zircaloy-4.
		ANT International, 2012

[40] This acronym implies that the fuel inspection revealed CRUD deposits on the fuel rod and that the deposits were uneven in the rod circumference.

Table 7-3: Summary of previous BWR failure key events, see previous ZIRAT/IZNA-reports for details.

Nuclear unit	Type of primary failure	Comment
KKL	1997, 1998	Excessive Shadow Corrosion on LK II Zr-2 Cladding under the Inconel x-750 grid springs. The oxide thickness was locally above 500 µm. The most notable cladding corrosion attacks were found on fuel that had experienced a fourth, fifth, or sixth operational cycle. Zn-injection. Low level of Fe in coolant.
River Bend	Cy 8, 1999	At least 12 GE First cycle FRs were failed. Heavy CRUD - The failures appeared in bundles with a significant iron CRUD deposition. The heavy deposits almost filled the gaps between the FRs. Some 700 pounds (320 kg) iron was estimated to have been input to the River Bend-1 RPV during cycle 8 (1998-1999). CRUD deposit thickness in the range 37–55 mils (940 – 1400 µm) was reported. Analysis of the CRUD showed that the major phases were hematite and spinel, reportedly magnetite or zinc ferrite. Significant amounts of copper, up to 15% were found in some cases. No NMCA. Zn-injection.
Vermont Yankee, 2001-2002	5 FRs failed due to CRUD corrosion.	A total of 5 failed GE rods in 4 bundles were removed from the core at Vermont Yankee in a mid-cycle outage in May 2002, along with 40 other bundles deemed most at risk of failure due to being similar to the leakers in terms of duty, exposure, and tubing material.
Browns Ferry 2, Cy 12, 2001-2003	63 FAs failed due to CRUD corrosion.	Affected fuel was GE13B claddings that failed in their second cycle with burnups of 29-30 MWd/kgU. Bundles that failed tended to be leading for the reload batch, indicating some impact of duty on tendency for failures. HWC started in BOC Cy 11 and NMCA at EOC 11 was implemented (3/01), Depleted Zinc Oxide (DZO) started in 1997 at 3 to 5 ppb. Maximum oxide thickness both in lower and upper part of the failed rods. Maximum CRUD deposition towards the bottom of the rods. BF-2 changed out their condenser tubes to Ti-tubes 8-10 years ago.
Browns Ferry 3, Cy 11, 2002-2004	3 FAs failed due to CRUD corrosion.	DZO started in 1995 at 3 to 5 ppb, NMCA at EOC 9 was implemented and HWC started in BOC Cy 10, DZO went to 5 to 10 ppb after the HWC was started. Affected fuel was GE13B claddings that failed in their third cycle with burnups of 43-47 MWd/kgU. Rod oxide thickness peaked at lower and upper part of the rods but maximum oxide thickness was found in upper part of the failed rods.
River Bend, Cy 11, 2003	7 rods failed due to CRUD related corrosion.	Water chemistry apparently within specification. Cy 11 - No NMCA but HWC and Zn-injection, also high Cu coolant content was observed. First cycle fuel with burnup ranging from 14.6-19.0 MWd/kgU. Siemens ATRIUM-10 (LTP). All failed rods were on periphery in FA on bladed surfaces (high power positions). Failures and peak oxide thicknesses in span 2 (of peripheral rods) where max. CRUD deposition was noted.
Hatch 1, Cy 21, 2003	PCI related failures in five (5) liner (barrier) FRs	Five duty related FRs failed at 19 months into a 22 month cycle in one cycle GE14 barrier fuel with an estimated burnup of 26 MWd/kgU.
Fitzpatrick, 2004	PCI related failures in two (2) non-barrier fuel	Two duty related failures occurred in non-barrier GE12 assemblies late in their second cycle at a burnup of about 45 MWd/kgU.

9 Fuel performance during dry storage (Charles Patterson)

9.1 Introduction

Managed, recoverable storage of irradiated fuel continues to be an essential aspect of water-reactor fuel cycles throughout the nuclear community. As of the latest comprehensive survey (mid-2010), about 225 000 tons of used or spent nuclear fuel (SNF)[52] is being stored around world [Sokolov, 2010]. The inventory of SNF is increasing by about 6 800 tons per year and is expected to reach ~445 000 tons by 2020, when current reactors reach the end of their operating lives [IAEA, 2008]. Estimates of SNF inventories at the end of 2010 are shown by country in Table 9-1.

Table 9-1: Estimated SNF inventories by country at the end of 2010 and by 2020, after [Peachy, 2012].

Country	SNF inventory (MTM)		Notes
	Current	Projected	
Belgium	---	5 000	
Canada	42 946	92 000	
Finland	1 820	5 500	
France	13 772		Active reprocessing program
Germany	6 801	10 800	Projected does not reflect current phase-out policy
Hungary	980	2 123	
Japan	16 714		March 2011; reprocessing program being developed
Korea	10 761	71 000	December 2009
Russia	19 240		Active reprocessing program
Sweden	5 818	12 000	
Switzerland	1 240	3 575	
UK	5 850		December 2007; reprocessing program
USA	65 000	130 000	
Ukrane	4 651		July 2008
			ANT International, 2012

Spent fuel is being stored in pools that are either located in reactor buildings or are located away from reactors and in dry containers at located at reactor sites or at interim storage facilities. In general, SNF is being stored successfully in wet and dry storage systems as shown in Table 9-2. Concern exists, however, with respect to the optimum roles of wet and dry storage due to damage to the buildings that housed the at-reactor spent fuel pools of the Fukushima Dai-ichi reactors following the Great Tohoku Earthquake and Tsunami in March 2011. Although initial reports of extensive SNF damage due to decay heat and pool boil-off appear to be unfounded [ANS, 2012], deliberations continue regarding the desirability of rapid transfers of spent fuel from storage pools to dry storage containers. Regardless of the outcome of these deliberations, managed storage is only a temporary step in the overall fuel cycle; the fundamental issue of post-storage processing and disposition of SNF and high-level waste (HLW) is being addressed differently among nuclear countries and remains unresolved other than agreement that geologic disposal is ultimately needed.

[52] The term "Spent Nuclear Fuel" is used collectively in this report to refer to nuclear fuel that is described in literature and regulations as either "used" or "spent". In this case, SNF refers to irradiated fuel that will be stored in a recoverable manner prior to reprocessing or permanent disposal regardless of its initial, post-discharge disposition.

Table 9-2: Spent fuel storage methods by country, after [Peachy, 2012].

Country	On-Site Storage			Centralized Storage		
	AR wet	AFR wet	Dry	Wet reprocessing	Wet aging	Dry
Argentina	X		X			
Armenia	X		X			
Belgium	X	X	X			
Brazil	X					
Bulgaria	X		X			
Canada	X		X			
China	X		X	X		
Czech Republic	X		X			
Finland	X	X(UC)				
France	X			X		
Germany	X		X			X
Hungary	X					X
India	X			X		X
Italy	X				X	
Japan	X	X	X	X		X(UC)
Korea	X		X			
Mexico	X					
Netherlands	X					
Pakistan	X					
Romania	X		X			
Russia	X			X	X	X
Slovakia	X	X				
Slovenia	X					
South Africa	X		X			
Spain	X		X			
Sweden	X				X	
Switzerland	X	X	X			X
Taiwan	X		X(UC)			
UK	X		X	X		
Ukrane	X		X			
USA	X		X			
Notes: AR = At reactor, AFR = Away from reactor, UC = Under construction						
ANT International, 2012						

Approaches to the fuel cycle vary among countries with nuclear power programs [Kakodkar, 2010]. Many countries have explicitly or implicitly (by indecision) adopted an open fuel cycle in which SNF will be disposed of in permanent repositories without recycling. Other countries have implemented or are developing recycling programs; e.g., China, France, India, Japan, Russia and the United Kingdom. In all cases, capabilities for interim storage and for the final disposal of SNF and the related HLW are needed. The various flow paths of SNF from discharge through interim storage and reprocessing or disposal is shown in Figure 9-1.

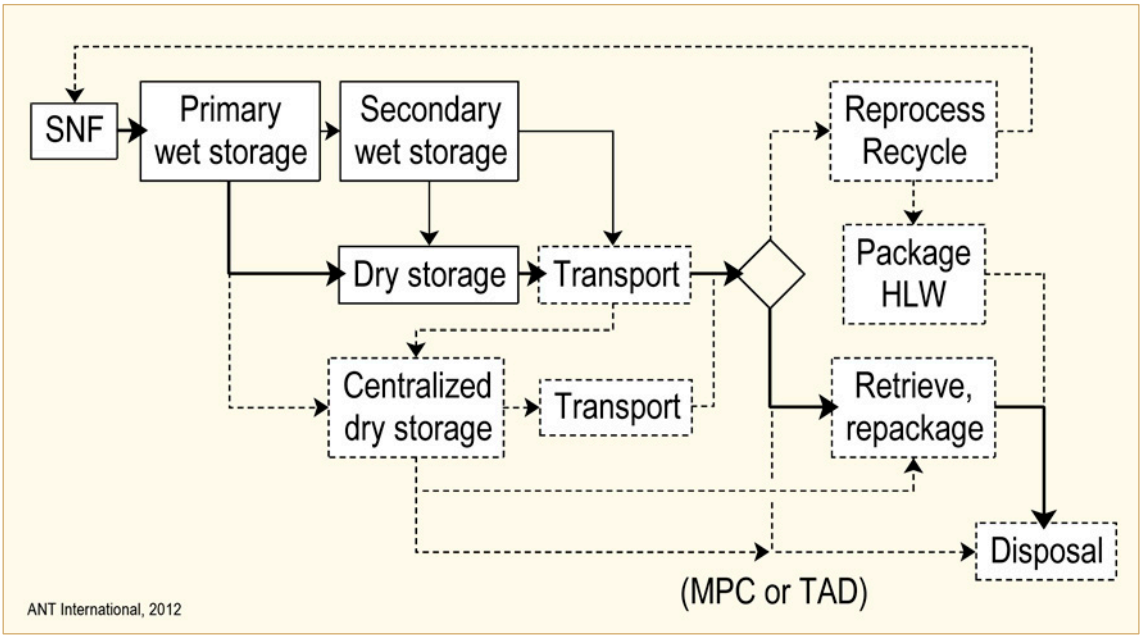

Figure 9-1: Flow paths of SNF and HLW from discharge to reprocessing or disposal.

Currently, large scale, commercial repositories for SNF and HLW are unavailable. Most countries that generate nuclear power are in the process of developing criteria, designs and sites for the permanent disposal of spent nuclear fuel. As indicated in Table 9-3, however, operating repositories have yet to become licensed realities. Meanwhile the pools at the nuclear plant sites are filling with spent fuel and the utilities are transferring the spent fuel from the pools to dry cask storage sites that are located, mostly, at the plant sites but also at remote storage facilities. As indicated in Table 9-2, exceptions to this practice are the central, large intermediate pool facilities that serve all the plants in Sweden (CLAB facility), all the plants in Finland (KPA-STORE), the fuel waiting reprocessing at La Hague, France and fuel from RBMK and VVER reactors in Russia. The lack of a licensed permanent fuel repository in any country has placed total reliance on intermediate storage. As a result dry storage has become a major activity and business component of current fuel strategies.

The importance of dry storage in back-end fuel strategies is due to a combination of factors. As noted above, the absence of permanent, geologic repositories combined with limited, in-pool storage capacity at reactor sites has forced the use of dry storage technology in countries that utilize a once-through, direct-disposal fuel cycle. Note that capabilities for interim storage will be needed even after permanent repositories become available because of storage limitations at existing reactor sites and likely constraints on decay heat in the repositories.

9.6 Summary

Progress is being made towards permanent repositories for SNF and HLW in some countries. Managed interim storage, however, remains an essential component in all commercial fuel cycles. Dry storage at reactor sites and at facilities located away-from-reactors continues to be the principal means for accommodating fuel assemblies that exceed the working capacities of fuel storage pools. All plants in the US either have or are planning to have dry storage facilities. Similar efforts involving combinations of wet and dry storage are taking place elsewhere.

In the US, the proposal by the "Blue Ribbon Commission on America's Nuclear Future" for the development of one or more centralized, dry storage facilities in conjunction with permanent disposal facilities is being discussed [BRC, 2012d]. Development of centralized storage facilities is projected to require 10-30 years. The Transportation and Storage Subcommittee of the BRC is also advocating lower density storage in spent fuel pools and earlier transfer to dry storage. This position restates early arguments against high storage densities and is motivated by the perception of conditions at the Fukushima Dai-ichi site following the earthquake and tsunami in March, 2011.

Due to delays in developing reprocessing and disposal capabilities, the length of time that SNF must remain in dry storage is increasing. The duration of dry storage licenses is being increased from 20 years to 40 years. The storage time is also increasing, with intervals ranging from 120-300 years now being considered.

Fuel now being discharged from LWRs in the US and other countries exceeds the high-burnup threshold (45 GWd/MTU) for storage, with increasing fractions of each reload approaching the 62 GWd/MTU limit imposed by the USNRC. Concerns related to dry storage stem both from extended storage and increased burnups. These concerns involve both SNF and the storage systems and are being addressed by new, ad hoc consortia. Technical gaps related to extended storage have been identified and are being assessed with respect to relative importance and potential sources of information.

The exposure of breached fuel rods to oxidizing environments poses risks relative to the retrieval or recovery of SNF. The risks come from the oxidation of exposed fuel pellets, degradation of the fuel matrix and fuel swelling strains that can fracture the cladding of the affected rods. The risk of oxidation is greatest during drying operations and the initial 10-15 years of storage when temperatures are high. The risk decreases with storage time due to the loss of decay heat and reduced temperatures. Issues associated with the confinement of oxidation products (U_3O_8 powder) are severe enough, however, to require careful consideration in plans for post-storage processing.

As discussed in earlier sections as BU and fluence become higher, material properties and microstructure evolve. Examples include:

- In PWRs it is found the Zry-4 no longer meets corrosion and hydriding needs; therefore virtually all current PWR cladding use a zirconium alloy containing Nb.
- Although not a new phenomena, observed SPP dissolution and re-precipitation phenomena have required a new perspective on alloy development and HPU.
- BWR channel bow at HB has required a new understanding of the relationships between HPU, shadow corrosion and irradiation growth.

A broader listing of issues needing resolution include:

- Corrosion related to oxide thickness and H pickup:
  - BWRs and PWRs:
    - Mechanism of solid hydrides on corrosion mechanism.
    - Effect of Nb.
  - BWRs:
    - Shadow corrosion mechanisms and its relation to channel bow.
    - Late increased corrosion and HPU of Zry-2 at HBs.
    - Localised hydriding – Browns Ferry –new failure mechanism
    - CRUD-chemistry-corrosion interaction.
    - Effect of water chemistry impurities, as well as specific effects of NMCA, with or without Zn-injection.
  - PWRs:
    - Effects of surface contaminations and/or boiling on Zr-Nb alloys.
    - Welding of the new alloys may need improved processes (Zr-Nb alloys).
    - Effect of increased Li together with increased duty (sub-cooled boiling) with and without Zn-injection.
    - Effects of increased hydrogen coolant content (to mitigate Primary Water Stress Corrosion Cracking (PWSCC)).
    - Axial offset anomaly (AOA) mechanisms.
- Mechanical properties related to irradiation and H pickup:
  - Decreased ductility and fracture toughness as consequence of the increased HPU and formation of radial hydrides during any situation (e.g., RIA, PCMI, LOCA and post-LOCA events, seismic event, transport container drop-accident conditions).
  - Quantification of the effect of irradiation on solubility of hydrogen, and mechanism by which the phenomenon occurs.
  - Details of deformation mechanisms in zirconium alloys, including being able to predict the dislocation channelling system.
  - Development of micromechanical models applicable to deformation at appropriate component conditions.
  - DHC mechanism (degradation of failed fuel, outside-in cracking and dry storage).
  - Role and kinetics of Fe, Cr, Ni from dissolving SPPs in Zry and Zr-Nb alloys for corrosion, mechanical properties and dimensional stability.

- Dimensional stability:
  - Effect of hydrogen on irradiation growth mechanisms.
  - PWR FA bowing mechanism.
  - BWR fuel channel bowing mechanism and parameters affecting it such as: texture, residual stress, flux gradient, hydrogen and hydrogen gradient.
  - Mechanism of <c> loop formation in zirconium alloys.
  - Mechanisms of both irradiation and post-irradiation creep.
  - Role of Nb in decreasing irradiation growth.
  - The effects of texture and HPU of Zr-Nb alloys as related to growth of PWR GTs.
  - Effects of thermal and radiation induced relaxation of Zr and Ni- alloys, particularly relative to SGs.
- PCI and PCMI:
  - PCMI failure mechanism during out-side in cracking, and possible relevance to failure mechanism for HB fuel?
  - Outside in-cracking both for BWR and PWR (new) claddings at high burnups
  - PCI failure mechanisms due to MPSs.
  - PCI mechanism and performance of liner/barrier and pellets with additives at HB.
- LOCA:
  - Verification of coolant blockage with real FRs in lattice design, related to maintenance of coolable geometry.
  - Mechanism of runaway oxidation in Russian E110 alloys.
  - Conditions when alpha-Zr layers are formed due to fuel-clad bonding.
- RIA:
  - Effects of hydride orientation, hydrogen distribution and hydrogen content on PCMI FC failure mechanism.
- Severe accidents:
  - Performance and phenomena when coolable geometry cannot be sustained.
- Intermediate dry storage:
  - Effects of the projected longer dry storage times before final disposal on hydride reorientation and its consequences during a cask drop accidents.
    - Effects of hydride orientation, hydrogen distribution and hydrogen content as well as temperature during cask drop accident.
  - Effects of irradiation on hydrogen solubility of various Zr alloys.
  - The effects of hydrogen, temperature, stress and time on DHC in relation to extended storage of current, HB fuel.

11 References

Adamson R. B., *Cyclic Deformation of Neutron Irradiated Copper*, Phil. Mag. 17, pp. 681, 1968.

Adamson R. B., *Irradiation Embrittlement and Creep in Fuel Cladding and Core Components*, Proceedings of BNES Conference, London, p. 305, 1972.

Adamson R. B., *Irradiation Growth of Zircaloy*, Zirconium in the Nuclear Industry, Third Conference, ASTM STP 633, pp. 326, 1977.

Adamson R. B., Tucker R. P. and Fidleris V., *High-Temperature Irradiation Growth in Zircaloy*, Zirconium in the Nuclear Industry, 5th Conference, ASTM STP 754, D. G. Franklin, Ed., American Society for Testing and Materials, 208-234, 1982.

Adamson R. B. and Bell W. L., *Effects of Neutron Irradiation and Oxygen Content on the Microstructure and Mechanical Properties of Zircaloy*, Microstructure and Mechanical Behaviour of Materials, Proceedings: Int'l Symposiums, Xian, China, October, 1985, EMAS, pp. 237-246, Warley, UK, 1986.

Adamson R. B., *Effects of Neutron Irradiation on Microstructure and Properties of Zircaloy*, Zirconium in the Nuclear Industry; Twelfth International Symposium, ASTM STP 1354, pp. 15-31, West Conshohocken, PA, 2000.

Adamson R. B. and Rudling P., *Dimensional Stability of Zirconium Alloys*, ZIRAT7/IZNA2 Special Topics Report, ANT International, Mölnlycke, Sweden, ANT International, 2002/2003.

Adamson R. B, Cox B., Garzarolli F., Strasser A. and Rudling P., *ZIRAT9/IZNA4 Annual Report*, ANT International, Mölnlycke, Sweden, 2004/2005.

Adamson R. B. and Cox B., *Impact of Irradiation on Material Performance*, ZIRAT10/IZNA5 Special Topics Report, ANT International, Mölnlycke, Sweden, 2005/2006.

Adamson R. B., *Recovery of Irradiation Damage by Posts-Irradiation Thermal Annealing-Relevance to Hydrogen Solubility and Dry Storage Issues*, EPRI Technical Report 1013446, June 2006.

Adamson R., Cox B., Davies J., Garzarolli F., Rudling P. and Vaidyanathan S., *Pellet-Cladding Interaction (PCI and PCMI)*, ZIRAT11/IZNA6, Special Topics Report, ANT International, Mölnlycke, Sweden, 2006/2007.

Adamson R., Garzarolli F., Cox B., Strasser A. and Rudling P., *Corrosion Mechanisms in Zirconium Alloys*, ZIRAT12/IZNA7 Special Topics Report, ANT International, Mölnlycke, Sweden, 2007/2008.

Adamson R. B, Garzarolli F. and Patterson C., *In-Reactor Creep of Zirconium Alloys*, ZIRAT14/IZNA9 Special Topical Report, ANT International, Mölnlycke, Sweden, 2009a.

Adamson R. B, Garzarolli F., Patterson C., Rudling P. and Strasser A., *ZIRAT14/IZNA9 Annual Report*, ANT International, Mölnlycke, Sweden, 2009b.

Adamson R. B., Zirconium Production and Technology: The Kroll Medal Papers 1975-2010, ASTM RPS2, ASTM I, West Conshohocken, PA, 2010.

Adamson R. B, Garzarolli F., Patterson C., Rudling P. Strasser A. and Coleman K., *ZIRAT15/IZNA10 Annual Report*, ANT International, Mölnlycke, Sweden, 2010.

Adamson R., Garzarolli F., Patterson C., Rudling P., Strasser A., Coleman K. and Lemaignan C., *ZIRAT16/IZNA11 Annual Report*, ANT International, Mölnlycke, Sweden, 2011.

Adroguier B., *Synthèse de l'Essai PHEBUS 215 P*, Rapport Technique IPSN/DERS/SAEREL-2/84, July 1984.

Aleshin Y. and Sparrow J., *WEC design experience to reduce IRI potential in susceptible cores*, Jahrestagung Kerntechnik, Dresden, 2009.

Alexander W. K., Fidleris V. and Holt R. A., *Zry-2 pressure tube elongation at the Hanford N Reactor*, ASTM Spec. Techn. Publ. 633), pp. 344-364, 1977.

Alvarez Holston A-M., Grigoriev V., Lysell G., Källström R., Johansson B., Hallstadius L., Zhou G., Arimescu I. and Lloret M., *A Combined Approach to Predict the Sensitivity of Fuel Cladding to Hydrogen-Induced Failures during Power Ramps*, Proceedings of 2010 LWR Fuel Performance/Top Fuel/WRFPM, Orlando, Florida, USA, September 26-29, 2010.

Anderson T., Almberger J and Björnkvist L., *A Decade of Assembly Bow Management at Ringhals*, ANS Topical Meeting on Light Water Reactor Fuel Performance, Orlando, Fl., 2004.

Andriambololona H. et al., *Methodology for a numerical simulation of an insertion or a drop of the rod cluster control assembly in a PWR*, Nuclear Engineering and Design 237, 600–606, 2007.

ANS, *Fukushima Daiichi: ANS Committee Report*, A Report by The American Nuclear Society Special Committee on Fukushima, American Nuclear Society, La Grange Park, Illinois, USA, 2012.

Arana I., Munoz-Reja C. and Culebras F., *Post-irradiation examination of high burnup fuel rods from Vandellos II*, Top Fuel Reactor Fuel Performance, Manchester, UK, 2012.

Arimescu I., Private communication, 2009.

Asatiani I., Balabanov S. and Kuznetsov A., *Operational Results of WWER Fuel* Fabricated *by MSZ, (Elektrostal, Russia)*, VVER Fuel Performance Conference, Helena Resort, Bulgaria, September, 2011.

Askeljung P., Flygare J. and Martinsson J., *NRC LOCA testing program at Studsvik, results on high burnup fuel*, 2011 Water Reactor Fuel Performance Meeting, Chengdu, China, Sept. 11-14, 2011.

Askeljung P., Flygare J. and Minghetti D., *NRC LOCA testing program at Studsvik, recent results on high burnup fuel*, Top Fuel, 2012.

Aulló M and Rabenstein W. D. *European Fuel Group Experience on Control Rod Insertion and Grid to Rod Fretting*, IAEA TC Meeting on Fuel Assembly Structural Behaviour, Cadarache - November 2004.

Aulló M., Garcia-Infanta J. and Chapin D., *Post Irradiation Examination of High Burnup Assemblies in Vandellos II*, LWR Fuel Performance Conference, Orlando, Florida, September, 2010.

Aulló M., Aleshin Y. and Messier J., *Reduction of fuel assembly bow with the RFA fuel*, Top Fuel, 2012.

B&W-Report, *Mk-B mechanical design report*, BAW-10172NP, 1989.

Barbéris P., Rebeyrolle V., Vermoyal J. J., Chabretou V. and Vassault J. P., *CASTA DIVTM: experiments and modelling of oxide induced deformation in nuclear components*, 15th ASTM International Symposium: Zirconium in the Nuclear Industry, Sunriver, OR, June 2007, SRP 1505, B. Kammenzind and M. Limbäck, eds., ASTM I, pp. 612-631, 2009.